In vivo mutagenicity and initiation following oxidative DNA lesion in the kidneys of rats given potassium bromate

Takashi Umemura,[1,4] Keita Kanki,[1] Yuichi Kuroiwa,[1] Yuji Ishii,[3] Keita Okano,[3] Takehiko Nohmi,[2] Akiyoshi Nishikawa[1] and Masao Hirose[1]

Divisions of [1]Pathology and [2]Genetics and Mutagenesis, National Institute of Health Sciences, 1-18-1 Kamiyoga, Setagaya-ku, Tokyo 158-8501; and [3]Faculty of Pharmaceutical Science, Department of Analytical Chemistry, Hoshi University, 2-4-41 Ebara, Shinagawa-ku, Tokyo 142-8501, Japan

(Received February 17, 2006/Revised April 21, 2006/Accepted May 1, 2006/Online publication June 29, 2006)

To clarify the role of 8-OHdG formation as a starting point for carcinogenesis, we examined the dose-dependence and time-course of changes of *OGG1* mRNA expression, 8-OHdG levels and *in vivo* mutations in the kidneys of *gpt* delta rats given $KBrO_3$ in their drinking water for 13 weeks. There were no remarkable changes in *OGG1* mRNA in spite of some increments being statistically significant. Increases of 8-OHdG occurred after 1 week at 500 p.p.m. and after 13 weeks at 250 p.p.m. Elevation of Spi$^-$ mutant frequency, suggestive of deletion mutations, occurred after 9 weeks at 500 p.p.m. In a two-stage experiment, F344 rats were given $KBrO_3$ for 13 weeks then, after a 2-week recovery, treated with 1% NTA in the diet for 39 weeks. The incidence and multiplicity of renal preneoplastic lesions in rats given $KBrO_3$ at 500 p.p.m. followed by NTA treatment were significantly higher than in rats treated with NTA alone. Results suggest that a certain period of time might be required for 8-OHdG to cause permanent mutations. The two-step experiment shows that cells exposed to the alteration of the intranuclear status by oxidative stress including 8-OHdG formation might be able to form tumors with appropriate promotion. (*Cancer Sci* 2006; 97: 829–835)

Oxidative DNA damage is caused by reactive oxygen species derived from various processes of cellular metabolism, especially metabolism of exogenous mutagens and carcinogens. 8-OHdG, a form of guanine oxidized at the C-8 position, is believed to be fairly stable and the most abundant oxidative lesion[1] among the many oxidized nucleosides known. It is established that 8-OHdG lesions are repaired mainly by the so-called GO system.[2] In this system: OGG1 DNA glycosylase and apurinic/apyrimidic lyase act to correct 8-OH-G:C pairs;[3] MYH glycosylase removes an A base mispaired with 8-OHdG;[4] and MTH 8-OH-dGTpase hydrolyzes 8-OH-dGTP in the nucleotide pool for prevention of its incorporation into DNA.[5] Thus, the existence of these three genes for repair of 8-OHdG in DNA points to 8-OHdG as a biologically deleterious base lesion. Induction of *OGG1* mRNA expression and an increase of OGG1 activity following application of exogenous oxidative stimuli have been demonstrated.[6–9]

$KBrO_3$, which induces renal cell tumors in F344 rats after oral administration at concentrations of 250 and 500 p.p.m,[10] has been classified as a genotoxic carcinogen based on positive mutagenicity in the Ames,[11] chromosome aberration,[12] and micronucleus[13] tests. Effective prevention of $KBrO_3$ clastogenicity by antioxidants,[14,15] and induction of 8-OHdG by $KBrO_3$ *in vitro* and *in vivo* strongly suggest that 8-OHdG plays a key role in $KBrO_3$ mutagenesis and carcinogenesis.[16–19] $KBrO_3$ has therefore received much attention as a suitable agent for research into 8-OHdG-related carcinogenesis. With a single dose of $KBrO_3$ by i.p. injection, 8-OHdG glycosylase activity in the rat kidney is increased in association with 8-OHdG formation.[20] A recent study using *OGG1*-deficient *gpt* delta mice found high amounts of 8-OHdG in the genome DNA and GC:TA transversion mutations following $KBrO_3$ exposure at a concentration of 2000 p.p.m. for 12 weeks.[21] However, a single high dose of $KBrO_3$ (300 mg/kg) did not induce tumors in rats,[22] and its carcinogenicity in mice is equivocal.[23] Therefore, interpretation of data for 8-OHdG and consequent mutations with reference to their significance for carcinogenesis is difficult.

Our aim is to determine conditions required for cells with 8-OHdG that survive specific repair systems to develop mutations and have tumor-initiating potential. For this purpose, carcinogenic doses of $KBrO_3$ were administered in drinking water and the dose-dependence and time-course of changes in *OGG1* mRNA expression, 8-OHdG levels and *in vivo* MFs in the kidneys of *gpt* delta rats were measured. In a second experiment, F344 rats were given NTA as a kidney tumor-promoter,[24] in a two-stage rat renal carcinogenesis experiment to assess tumor-initiation activity of $KBrO_3$ given at the same doses as in the first experiment.

Materials and methods

Chemicals

$KBrO_3$ and NTA were purchased from Wako Pure Chemical Industries (Osaka, Japan) and Tokyo Kasei (Tokyo, Japan),

[4]To whom correspondence should be addressed. E-mail: umemura@nihs.go.jp

Abbreviations: 6-TG, 6-thioguanine; 8-OHdG, 8-hydroxydeoxyguanosine; AHs, atypical hyperplasias; ATs, atypical tubules; BD, basal diet; H–E, hematoxylin–eosin; $KBrO_3$, potassium bromate; dG, deoxyguanosine; DW, distilled water; MFs, mutant frequencies; NTA, nitrilotriacetic acid trisodium salt; PCR, polymerase chain reaction; p.p.m., parts per million; RCTs, renal cell tumors; SD, standard deviation.

doi: 10.1111/j.1349-7006.2006.00248.x

respectively. Alkaline phosphatase was obtained from Sigma Chemical (St. Louis, MO, USA) and nuclease P1 was from Yamasa Shoyu (Chiba, Japan).

Animals, diet and housing conditions

The protocol for this study was approved by the Animal Care and Utilization Committee of the National Institute of Health Sciences (Tokyo, Japan). Five-week-old male *gpt* delta rats carrying approximately 10 tandem copies of the transgene lambda EG10 per haploid genome and F344 rats were obtained from Japan SLC (Shizuoka, Japan) and from Charles River Japan (Kanagawa, Japan), respectively. They were housed in polycarbonate cages (five rats per cage) with hardwood chips for bedding in a conventional animal facility, maintained under conditions of controlled temperature (23 ± 2°C), humidity (55 ± 5%), air change (12 times per hour), and lighting (12 h light/dark cycle) and were given free access to CRF-1 BD (Charles River Japan) and tap water.

Animal treatment

Experiment I. Groups of five male gpt delta rats were given $KBrO_3$ solution at concentrations of 0, 60, 125, 250 and 500 p.p.m. in the drinking water for 13 weeks. Additional subgroups of five male *gpt* delta rats were given $KBrO_3$ solution at a dose of 500 p.p.m. in the drinking water for 1, 5 or 9 weeks. At the end of each period, the animals were killed under ethyl ether anesthesia and a part of one kidney was homogenized in Isogen (Nippon Gene, Tokyo, Japan) and stored at −80°C until used for isolation of total RNA. The remaining kidney was also stored at −80°C for 8-OHdG measurement and *in vivo* mutation assays.

Experiment II. F344 rats were used in the tumor initiation study rather than Sprague–Dawley rats, a back strain of *gpt* delta rats, because of the accumulated data on the effects of $KBrO_3$ on the former strain. Ninety F344 male rats were randomly divided into seven groups. Fifteen animals each in groups 2–5 were given $KBrO_3$ at concentrations of 60, 125, 250 and 500 p.p.m. for 13 weeks. After a 2-week recovery period, rats received NTA as a promoter at a concentration of 1% in the diet for 37 weeks. Ten animals each in groups 1 and 6 were given DW in place of $KBrO_3$, followed by the NTA regimen at doses of 0 and 1%, respectively. Additionally, 10 animals in group 7 were maintained untreated following $KBrO_3$ treatment at a concentration of 500 p.p.m. for 13 weeks until the end of the experiment. Rats were killed at week 52 under ethyl ether anesthesia and the kidneys were removed immediately and fixed in 10% buffered formalin.

Real-time reverse transcription–PCR for mRNA of *OGG1*

Total mRNA was isolated using the Isogen total mRNA isolation reagent (Nippon Gene) according to the manufacturer's instructions. After reverse-transcription with random hexamers using an SYBR RT-PCR Kit (Takara Bio, Shiga, Japan), PCR was carried out with specific primers for rat *OGG1* (5′-CAACATTGCTCGCATCACTGG-3′ and 5′-ATGGCTTTAGCACTGGCACATACA-3′) (Smart Cycler; Cepheid, Sunnyvale, CA) and r*GAPDH* (5′-GACAACTTTG-GCATCGTGGA-3′ and 5′-ATGCAGGGATGATGTTCTGG-3′) (Ex Taq, RT-PCR version; Takara Bio). Real-time monitoring of PCR products was achieved with fluorescence of SYBR green I (Takara Bio), and expression levels of *OGG1* were determined as ratios to *GAPDH* levels obtained with the same master reaction.[25] All of the procedures after isolation of total RNA were carried out at the Dragon Genomics Center of Takara Bio (Mie, Japan).

Measurement of nuclear 8-OHdG

In order to prevent 8-OHdG formation as a by-product during DNA isolation,[26] kidney DNA was extracted using a slight modification of the method of Nakae *et al.*[27] Briefly, nuclear DNA was extracted with a commercially available DNA Extracter WB Kit (Wako Pure Chemical Industries) containing an antioxidant NaI solution to dissolve cellular components. For further prevention of auto-oxidation in the cell lysis step, deferoxamine mesylate (Sigma Chemical) was added to the lysis buffer.[28] The DNA was digested to deoxynucleotides with nuclease P1 and alkaline phosphatase and levels of 8-OHdG (8-OHdG/10^5 dG) were measured by high-performance liquid chromatography with an electrochemical detection system (Coulochem II; ESA, Bedford, MA).

In vivo mutation assays

6-TG and Spi$^-$ (insensitive P2 interference) selection was carried out as previously described.[29] Briefly, genomic DNA was extracted from the kidneys, and lambda EG10 DNA (48 kb) was rescued as the lambda phage by *in vitro* packaging. For 6-TG selection, the packaged phage was incubated with *Escherichia coli* YG6020, expressing Cre recombinase, and converted to a plasmid carrying *gpt* and chloramphenicol acetyltransferase. Infected cells were mixed with molten soft agar and poured onto agar plates containing chloramphenicol and 6-TG. In order to determine the total number of rescued plasmids, infected cells were also poured on plates containing chloramphenicol without 6-TG. The plates were incubated at 37°C for the selection of 6-TG-resistant colonies, and the *gpt* MF was calculated by dividing the number of *gpt* mutants after clonal correction by the number of rescued phages.

For Spi$^-$ selection, the packaged phage was incubated with *E.coli* XL-1 Blue MRA for survival titration and *E.coli* XL-1 Blue MRA P2 for mutant selection. Infected cells were mixed with molten lambda-trypticase soft agar and poured onto lambda-trypticase agar plates. The plaques (Spi$^-$ candidates) detected on the plates were suspended in SM buffer. In order to confirm the Spi$^-$ phenotype of candidates, the suspensions were spotted on three types of plates containing XL-1 Blue MRA, XL-1 Blue MRA P2, or WL95 P2 strains and were spread with soft agar. The numbers of mutants that made clear plaques on each plate were counted as confirmed Spi$^-$ mutants. The Spi$^-$ MF was calculated by dividing the number of Spi$^-$ mutants by the number of rescued phages.

Histopathology for the initiation bioassay

Formalin-fixed kidneys were processed for embedding in paraffin and sectioned at 2 μm. Sections were routinely stained with H–E for histopathological assessment. All sections were coded and read without knowledge of the treatment for counting of ATs, AHs and RCTs. The

doi: 10.1111/j.1349-7006.2006.00248.x

diagnostic criteria for preneoplastic and neoplastic lesions of the kidney proposed by Dietrich and Swenberg,[30] were used to distinguish ATs, AHs and RCTs.

Statistics

The significance of differences in the results for mRNA levels of *OGG1*, 8-OH-dG levels and MFs was evaluated with ANOVA, followed by Dunnett's multiple comparison test. The significance of differences in the multiplicity of lesions in the initiation bioassay was evaluated using Tukey's test, and that for incidences with Fisher's exact probability test.

Results

Experiment I

OGG1 *mRNA expression.* Figure 1(a) illustrates changes of *OGG1* mRNA expression in kidneys of *gpt* delta rats given $KBrO_3$ solution at concentrations of 0, 60, 125, 250 and 500 p.p.m. in the drinking water for 13 weeks. Significant ($P < 0.05$) elevation of expression occurred at 250 p.p.m. At 500 p.p.m., a significant increase of expression ($P < 0.01$) was evident 5 weeks after the start of the exposure (Fig. 1b).

8-OHdG levels. Figure 2(a) shows data for 8-OHdG levels in kidneys of *gpt* delta rats given $KBrO_3$ in the drinking water for 13 weeks. 8-OHdG levels were elevated compared to the control value (0.28 ± 0.06 8-OHdG/10^5 dG) at $KBrO_3$ concentrations of 250 and 500 p.p.m. in a clearly dose-dependent manner (250 p.p.m., 0.45 ± 0.19 8-OHdG/10^5 dG, $P < 0.05$; 500 p.p.m., 0.59 ± 0.16 8-OHdG/10^5 dG, $P < 0.01$). Figure 2(b) summarizes the data from kidneys of *gpt* delta rats given $KBrO_3$ solution at a concentration of 500 p.p.m. for 1, 5, 9 and 13 weeks. 8-OHdG levels increased with time, with a peak at week 5 and a gradual decrease thereafter. All of the 8-OHdG levels for the treated rats were statistically significant ($P < 0.01$) compared to the control value (1 week, 0.54 ± 0.10 8-OHdG/10^5 dG; 5 weeks, 0.88 ± 0.10 8-OHdG/10^5 dG; 9 weeks, 0.75 ± 0.02 8-OHdG/10^5 dG).

In vivo *mutations.* Changes in *gpt* and Spi$^-$ MFs in *gpt* delta rats given $KBrO_3$ solution for 13 weeks are shown in Figs 3 and 4. There was no statistically significant increment in *gpt* MFs among the treated animals in spite of the dose-dependent increase of 8-OHdG observed in rats treated with 250 p.p.m. $KBrO_3$ (Fig. 3a,b). In contrast, Spi$^-$ MF in rats

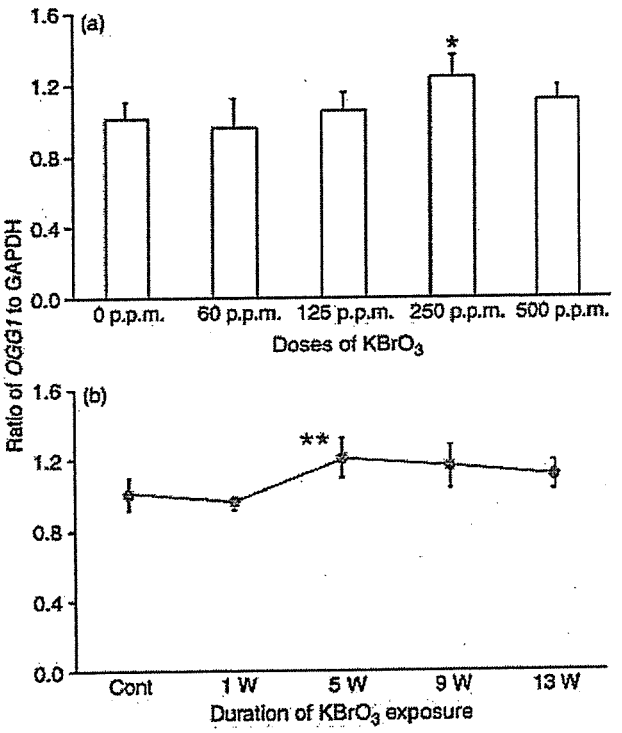

Fig. 1. (a) Dose-dependent expression of *OGG1* mRNA in kidneys of *gpt* delta rats given $KBrO_3$ at concentrations of 0, 60, 125, 250 and 500 p.p.m. in their drinking water for 13 weeks. Values are means ± SD of data for five rats. $*P < 0.05$, significantly different from the controls (0 p.p.m.). (b) Time-course of changes in expression of *OGG1* mRNA in kidneys of *gpt* delta rats given $KBrO_3$ at a concentration of 500 p.p.m. in their drinking water for 1, 5, 9 and 13 weeks. The values at 0 and 500 p.p.m. in the dose–response study were used as the control and 13-week values, respectively. Means ± SD of data for five rats are given. $**P < 0.01$, significantly different from the controls.

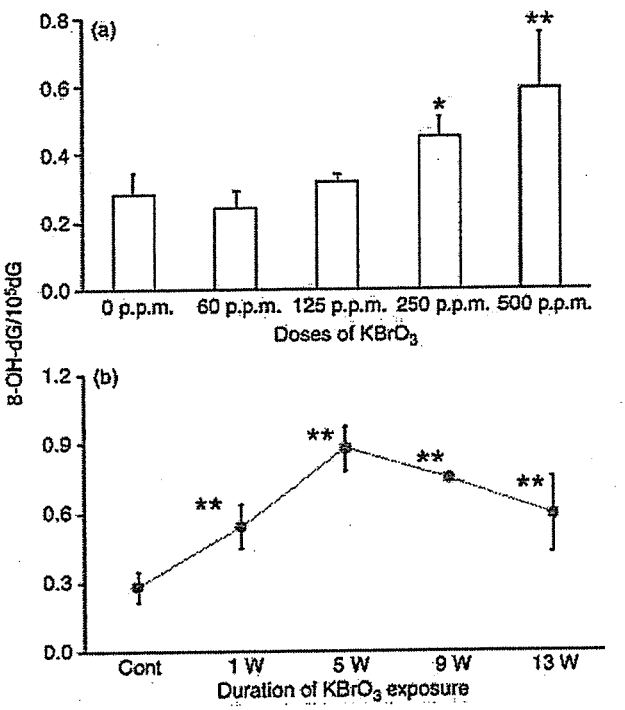

Fig. 2. (a) Dose-dependent induction of 8-OHdG in kidney DNA of *gpt* delta rats given $KBrO_3$ at concentrations of 0, 60, 125, 250 and 500 p.p.m. in their drinking water for 13 weeks. Values are means ± SD of data for five rats. $*P < 0.01$, $**P < 0.05$, significantly different from the controls (0 p.p.m.). (b) Time course of changes in levels of 8-OHdG in kidneys of *gpt* delta rats given $KBrO_3$ at a concentration of 500 p.p.m. in their drinking water for 1, 5, 9 and 13 weeks. The values at 0 and 500 p.p.m. in the dose–response study were used as the control and 13-week values, respectively. Means ± SD of data for five rats are given. $**P < 0.01$, significantly different from the controls.

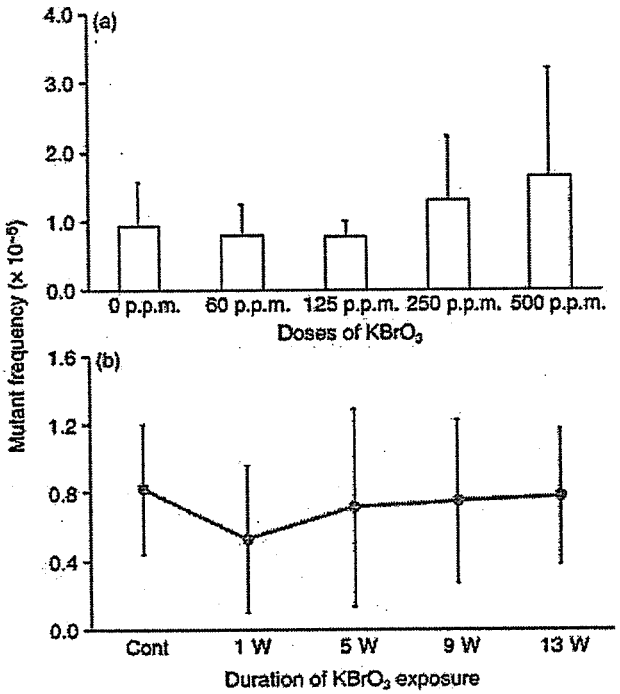

Fig. 3. (a) Dose–response data for *gpt* MFs in kidneys of *gpt* delta rats given $KBrO_3$ at concentrations of 0, 60, 125, 250 and 500 p.p.m. in their drinking water for 13 weeks. Values are means ± SD of data for five rats. (b) Time-course of changes in *gpt* MFs in kidneys of *gpt* delta rats given $KBrO_3$ at a concentration of 500 p.p.m. in their drinking water for 1, 5, 9 and 13 weeks. The values for controls and 13 weeks were obtained from re-analysis of the samples at 0 and 500 p.p.m., respectively, in the dose–response study. Values are means ± SD of data for five rats.

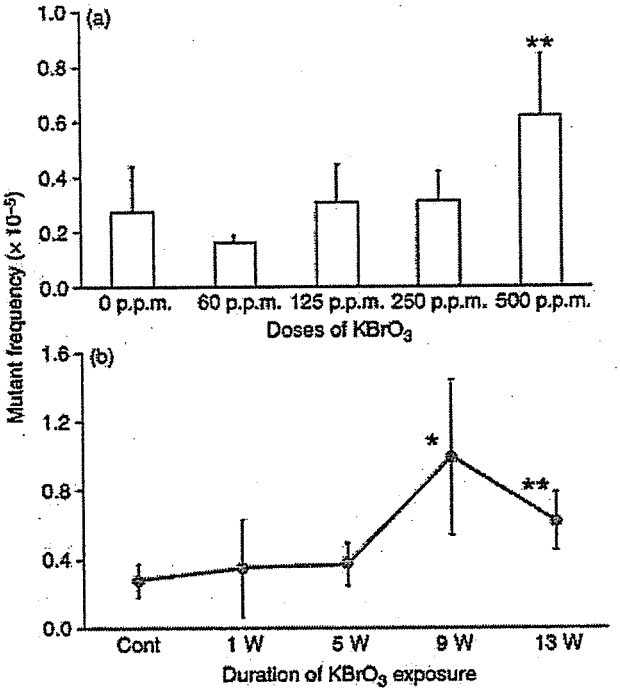

Fig. 4. (a) Dose–response data for Spi^- MFs in kidneys of *gpt* delta rats given $KBrO_3$ at concentrations of 0, 60, 125, 250 and 500 p.p.m. in their drinking water for 13 weeks. Values are means ± SD of data for five rats. $^{**}P < 0.01$, significantly different from the controls (0 p.p.m.). (b) Time-course of changes in Spi^- MFs in kidneys of *gpt* delta rats given $KBrO_3$ at a concentration of 500 p.p.m. in their drinking water for 1, 5, 9 and 13 weeks. The values for the controls and at 13 weeks were obtained from re-analysis of the samples at 0 and 500 p.p.m., respectively, in the dose–response study. Values are means ± SD of data for five rats. $^{*}P < 0.05$, $^{**}P < 0.01$, significantly different from the controls.

treated with 500 p.p.m. $KBrO_3$ was significantly higher ($P < 0.01$) than in untreated control rats (Fig. 4a). As shown in Fig. 4(b), a significant ($P < 0.05$) elevation of Spi^- MF appeared 9 weeks after the start of the exposure.

Experiment II

One animal given $KBrO_3$ at a dose of 250 p.p.m. followed by NTA treatment died of a malignant pheochromocytoma 49 weeks after the start of the experiment and was eliminated from the dataset. Final body weights were 391.3 ± 19.2 g (DW/BD), 3705 ± 23.2 g ($KBrO_3$ 60 p.p.m./NTA), 365.4 ± 18.5 g ($KBrO_3$ 125 p.p.m./NTA), 367.7 ± 26.6 g ($KBrO_3$ 250 p.p.m./NTA), 348.7 ± 20.1 g ($KBrO_3$ 500 p.p.m./NTA, $P < 0.01$ *versus* DW/BD), 360.2 ± 17.0 g (DW/NTA, $P < 0.05$ *versus* DW/BD) and 384.2 ± 18.4 g ($KBrO_3$ 500 p.p.m./BD). The incidences and multiplicities of renal preneoplastic lesions in rats given $KBrO_3$ at various doses for 13 weeks followed by NTA treatment are shown in Table 1. In all of the groups except the no-treatment control group, preneoplastic lesions were found (Fig. 5a,b). The multiplicity ($P < 0.01$) of ATs, and the incidence ($P < 0.05$) and multiplicity ($P < 0.05$) of AHs in rats given $KBrO_3$ at a dose of 500 p.p.m. followed by NTA were significantly elevated as compared with the values for rats given NTA only. A cystic adenoma was observed in a rat given $KBrO_3$ at the dose of 500 p.p.m. for 13 weeks followed by no-treatment for 39 weeks (Fig. 5c). However, there were no neoplastic lesions in any of the other groups.

Discussion

OGG1 mRNA levels have been found to be elevated in rat lungs after exposure to diesel exhaust particles,[6] in rat kidney after ischemic-reperfusion injury,[7] and in human lung alveolar epithelial cells following crocidolite asbestos treatment.[31] Because overexpression in these cases occurred concomitantly with an increment in OGG1 activity, it has been considered that the elevation in *OGG1* gene expression is linked with the increase of OGG1 activity,[31] and formation of 8-OHdG is a trigger for induction of OGG1 activity.[32–34] However, in the present study, overexpression of *OGG1* mRNA in the kidneys of rats given $KBrO_3$ was not demonstrated. It has been reported that OGG1 activities in the kidneys of rats given $KBrO_3$ by single i.p. injection at a dose of 80 mg/kg were increased in a time- and dose-dependent manner.[20] Also, a recent report showed that $KBrO_3$ exposure at a dose of 400 p.p.m. in drinking water for 52 weeks was able to induce an approximately fourfold increase in *OGG1* mRNA expression.[35] Therefore, chronic exposure to $KBrO_3$

doi: 10.1111/j.1349-7006.2006.00248.x

Table 1. Incidence and multiplicity data for preneoplastic lesions in the kidneys of rats given $KBrO_3$ at various doses followed by NTA treatment

Exposure	Number of rats at risk	Atypical tubules		Atypical hyperplasias	
		Incidence (%)	Multiplicity (number/rat)	Incidence (%)	Multiplicity (number/rat)
DW/BD	10	0	0.0	0	0.0
$KBrO_3$ (60 p.p.m)/NTA	15	93	3.1 ± 1.8	27	0.3 ± 0.6
$KBrO_3$ (125 p.p.m)/NTA	15	87	3.0 ± 2.9	27	0.3 ± 0.6
$KBrO_3$ (250 p.p.m)/NTA	14	100	3.7 ± 1.6	36	0.4 ± 0.6
$KBrO_3$ (500 p.p.m)/NTA	15	100	10.1 ± 4.5**	80*	1.3 ± 1.1*
DW/NTA	10	80	2.2 ± 1.5	30	0.4 ± 0.7
$KBrO_3$ (500 p.p.m)/BD	10	50	0.9 ± 1.1	20	0.2 ± 0.4

$KBrO_3$ was given in the drinking water for 13 weeks. NTA was given at a dose of 1% in the diet for 37 weeks. *$P < 0.05$, ** $P < 0.01$ *versus* DW/NTA.

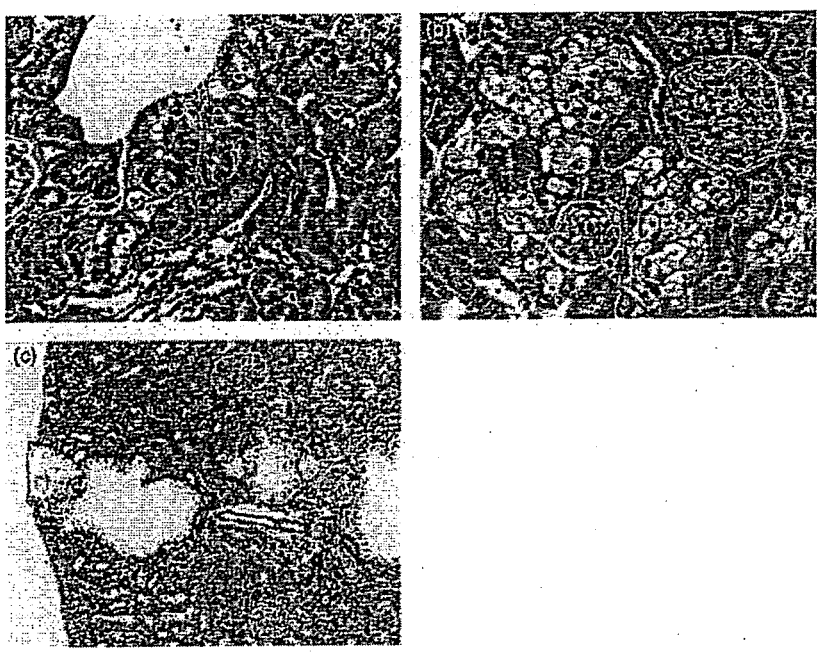

Fig. 5. (a) A single atypical tubule of basophilic cells in a rat treated with KBrO3 at a concentration of 500 p.p.m. in the drinking water for 13 weeks then, after a 2-week rest period, NTA at a concentration of 1% in the diet for 37 weeks. H–E stain. Original magnification × 80. (b) A focus of atypical hyperplasia composed of several atypical tubules, showing a solid structure and clear cell morphology in a rat treated with KBrO3 at a concentration of 500 p.p.m. in the drinking water for 13 weeks then, after a 2-week rest period, NTA at a concentration of 1% in the diet for 37 weeks. H–E stain. Original magnification × 80. (c) Cystic adenoma in a rat treated with $KBrO_3$ at a concentration of 500 pm in the drinking water for 13 weeks followed by no further treatment for 39 weeks. H–E stain. Original magnification × 33.

at carcinogenic levels for 9 weeks might be insufficient for affecting *OGG1* mRNA level.

Even though sustained increases in 8-OHdG formation were apparent through the experimental period, 9 weeks was needed to induce a significant increase of MF. In addition, the MF in the kidneys of rats given $KBrO_3$ at a dose of 250 p.p.m. did not change, despite statistically significant elevated 8-OHdG levels. Accordingly, the present data suggest that a period of time might be necessary for cells having high amounts of 8-OHdG to harbor mutations. This time factor might account for a previous bioassay finding of no initiating effects in rats given $KBrO_3$ by gavage as a single dose of 300 mg/kg, which is sufficient to increase 8-OH-dG levels in kidney DNA, and subsequently subjected to a promoting regimen for 102 weeks.[22]

In the present study, although we failed to detect an increase of *gpt* MF, significant elevation of *red/gam* MF, mainly attributable to deletion mutations, was found. Although it remains uncertain whether the mutation observed in *gpt* delta rats exposed to $KBrO_3$ originates in 8-OHdG, there have been several reports that formation of high amounts of 8-OHdG *in vivo* resulted in several types of mutations, including deletion mutations, besides GC:TA transversions. Previous work with *OGG1* knockout mice demonstrated that surprisingly high amounts of 8-OHdG due to $KBrO_3$ exposure resulted in an increase of deletion mutations and GC:AT transitions as well as GC:TA transversions.[21,36,37] Whereas mutations in NIH3T3 cells transfected with the *ras* gene, which incorporated 8-OHdG at the first position of codon 12, showed mainly GC:TA transversions, incorporation at the second position elicited GC:AT transitions to an appreciable extent.[36,38] Thus, the overall data indicate that mutations other than GC:TA transversions induced by 8-OHdG *in vivo* are possible.[39,40] Additionally, it is highly probable that other oxidized bases, such as 5-formyluracil and 5-hydroxycytosine,[41,42] were generated concomitantly with 8-OHdG formation. The

fact that deletion mutations were predominant among *p15* or *p16* lesions found in renal cell tumors induced by ferric nitrilotriacetate, an agent causing oxidative stress,[43] allows us to speculate that there might be certain types of DNA lesions related to oxidative stress that mainly cause deletion mutations.

The initiation bioassay clearly showed that a 13-week exposure to $KBrO_3$ at 500 p.p.m. was sufficient to induce renal preneoplastic lesions with significant incidence and multiplicity when followed by a typical renal tumor-promoter. Although $KBrO_3$ promotion activity has already been demonstrated in the kidneys of F344 rats when given in their drinking water,[23,44,45] this is the first report showing $KBrO_3$ initiating activity using the two-stage rat renal carcinogenesis model. Because Sprague–Dawley are a back strain of *gpt* delta rats, it seems hard to extrapolate their data to the results obtained from F344 rats. However, in addition to the fact that exposure of F344 rats to $KBrO_3$ at concentrations of 250 and 500 p.p.m. in their drinking water, not at 125 p.p.m. and below, was able to cause increase of 8-OHdG formation,[18] the initiation activity was found in the same dose-dependent fashion as *in vivo* mutagenicity in *gpt* delta rats. Further studies using newly developed *gpt* delta rats of F344 strain are now ongoing. In any case, based on the accumulated data using F344 rats it has been accepted that there is a close link between oxidative DNA damage and $KBrO_3$ carcinogenesis.[46] Considering that the increase of 8-OHdG implies occurrence of intranuclear oxidative stress, the present data suggest that the alteration of the intranuclear circumstances by oxidative stress might have the initiating potential.

In conclusion, the overall data suggest that not only the amount of 8-OHdG but also a period of time with high 8-OHdG levels might be required to bring an oxidized base lesion to mutation status. They also showed a possibility of cells with oxidative DNA damage becoming neoplastic under the influence of an appropriate tumor-promoter.

Acknowledgments

We thank Mss. Machiko Maeda, Ayako Kaneko and Mikiko Takagi for expert technical assistance in carrying out the animal experiments and processing histological materials. This work was supported in part by a Grant-in-Aid for Cancer Research from the Ministry of Health, Labor and Welfare of Japan.

References

1 Kasai H, Nishimura S. Formation of 8-hydroxydeoxyguanosine in DNA by oxygen radicals and its biological significance. In: Sies H. *Oxidative Stress: Oxidants and Antioxidants*. London: Academic Press, 1991; 99–116.
2 Michaels ML, Pham L, Cruz C, Miller JH. MutM, a protein that prevents G.C.-T.A. transversions, is formamidopyrimidine-DNA glycosylase. *Nucleic Acids Res* 1991; **19**: 3629–32.
3 Aburatani H, Hippo Y, Ishida T *et al.* Cloning and characterization of mammalian 8-hydroxyguanine-specific DNA glycosylase/apurinic, apyrimidic lyase, a function mutM homologue. *Cancer Res* 1997; **57**: 2151–6.
4 Zharkov DO, Grollman AP. MutY DNA glycosylase: base release and intermediate complex formation. *Biochemistry* 1998; **37**: 12384–94.
5 Fujikawa K, Kamiya H, Yakushiji H, Fujii Y, Nakabeppu Y, Kasai H. The oxidized forms of dATP are substrates for the human MutT homologue, the hMTHi protein. *J Biol Chem* 1999; **274**: 18201–5.
6 Tsurudome Y, Hirano T, Yamamoto H *et al.* Changes in levels of 8-hydroxyguanine in DNA, its repair and *OGG1* mRNA in rat lungs after intratracheal administration of diesel exhaust particles. *Carcinogenesis* 1999; **20**: 1573–6.
7 Tsuruya K, Furuichi M, Tominaga Y *et al.* Accumulation of 8-oxoguanine in the cellular DNA and the alteration of the *OGG1* expression during ischemic-reperfusion injury in the rat kidney. *DNA Repair* 2003; **2**: 211–29.
8 Yamaguchi R, Hirano T, Asami S, Chung M-H, Sugita A, Kasai H. Increased 8-hydroxyguanine levels in DNA and its repair activity in rat kidney after administration of a renal carcinogen, ferric nitrilotriacetate. *Carcinogenesis* 1996; **17**: 2419–22.
9 Lee M-R, Kim S-H, Cho H-J *et al.* Transcription factors NF-YA regulate the induction of human OGG1 following DNA-alkylating agent methylmethane sulfonate (MMS) treatment. *J Biol Chem* 2004; **279**: 9857–66.
10 Kurokawa Y, Hayashi Y, Maekawa A, Takahashi M, Kokubo T. Induction of renal tumors in F344 rats by oral administration of potassium bromate, a food additive. *Jpn J Cancer Res* 1982; **73**: 335–8.
11 Ishidate M, Sofuni T, Yoshioka K *et al.* Primary mutagenicity screening of food additives currently used in Japan. *Food Chem Toxicol* 1984; **22**: 623–36.
12 Ishidate M, Yoshioka K. Chromosome aberration tests with Chinese hamster cells *in vitro* with and without metabolic activation: a comparative study on mutagens and carcinogens. *Arch Toxicol Supplement* 1980; **4**: 41–4.
13 Hayashi M, Kishi M, Sofuni T, Ishidate M. Micronucleus tests with mice on 39 food additives and 8 miscellaneous chemical substances. *Chem Toxicol* 1988; **26**: 487–500.
14 Sai K, Uchiyama S, Ohno Y, Hasegawa R, Kurokawa Y. Generation of active oxygen species *in vitro* by the interaction of potassium bromate with rat kidney cells. *Carcinogenesis* 1992; **13**: 333–9.
15 Sai K, Takagi A, Umemura T, Hasegawa R, Kurokawa Y. The protective role of glutathione, cysteine and vitamin C against oxidative DNA damage induced in rat kidney by potassium bromate. *Jpn J Cancer Res* 1992; **83**: 45–51.
16 Ballmaier D, Epe B. Oxidative DNA damage induced by potassium bromate under cell-free conditions and in mammalian cells. *Carcinogenesis* 1995; **16**: 335–42.
17 Kasai H, Nishimura S, Kurokawa Y, Hayashi Y. Oral administration of the renal carcinogen, potassium bromate, specifically produces 8-hydroxydeoxyguanosine in rat kidney target organ DNA. *Carcinogenesis* 1987; **8**: 1959–61.
18 Umemura T, Kitamura Y, Kanki K *et al.* Dose-related changes of oxidative stress and cell proliferation in kidneys of male and female F344 rats exposed to potassium bromate. *Cancer Sci* 2004; **95**: 393–8.
19 Umemura T, Sai K, Takagi A, Hasegawa R, Kurokawa Y. A possible role for cell proliferation in potassium bromate ($KBrO_3$) carcinogenesis. *J Cancer Res Clin Oncol* 1993; **119**: 463–9.
20 Lee Y-S, Choi J-Y, Park M-K, Choi E-M, Kasai H, Chung M-H. Induction of oh8Gua glycosylase in rat kidneys by potassium bromate ($KBrO_3$), a renal oxidative carcinogen. *Mutat Res* 1996; **364**: 227–33.
21 Arai T, Kelly VP, Minowa O, Noda T, Nishimura S. High accumulation of oxidative DNA damage, 8-hydroxyguanine, in *Mmh/OGG1* deficient mice by chronic oxidative stress. *Carcinogenesis* 2002; **23**: 2005–10.
22 Kurata Y, Diwan BA, Ward JM. Lack of renal tumor initiating activity of a single dose of potassium bromate, a genotoxic renal carcinogen in male F344/NCr rats. *Food Chem Toxicol* 1992; **30**: 251–9.
23 Kurokawa Y, Maekawa A, Takahashi M, Hayashi Y. Toxicity and carcinogenicity of potassium bromate – a new renal carcinogen. *Environ Health Perspect* 1990; **87**: 309–35.
24 Hiasa Y, Kitahori Y, Konishi N, Shimoyama T. Dose-related effect of trisodium nitriloacetate monohydrate on renal tumorigenesis initiated with *N*-ethyl-*N*-hydroxyethyl-nitrosamine in rats. *Carcinogenesis* 1985; **6**: 907–10.
25 Nagata M, Fujita H, Ida H *et al.* Identification of potential biomarkers of lymph node metastasis in oral squamous cell carcinoma by cDNA microarray analysis. *Int J Cancer* 2003; **106**: 683–9.
26 Kasai H. Chemistry-based studies on oxidative DNA damage: formation, repair, and mutagenesis. *Free Rad Biol Med* 2002; **33**: 450–6.
27 Nakae D, Mizumoto Y, Kobayashi E, Noguchi O, Konishi Y. Improved genomic/nuclear DNA extraction for 8-hydroxydeoxyguanosine analysis of small amounts of rat liver tissue. *Cancer Lett* 1995; **97**: 233–9.
28 Helbock HJ, Beckman KB, Shigenaga MK *et al.* DNA oxidation matters:

doi: 10.1111/j.1349-7006.2006.00248.x

the HPLC-electrochemical detection assay of 8-oxo-deoxyguanosine and 8-oxo-guanine. *Proc Natl Acad Sci USA* 1998; **95**: 288–93.
29 Kanki K, Nishikawa A, Masumura K *et al. In vivo* mutational analysis of liver DNA in *gpt* delta transgenic rats treated with the hepatocarcinogens *N*-nitrosopyrrolidine, 2-amino-3-methylimidazo[4,5-*f*]quinoline, and di(2-ethylhexyl)phthalate. *Mol Carcinog* 2005; **42**: 9–17.
30 Dietrich DR, Swenberg JA. Preneoplastic lesions in rodent kidney induced spontaneously or by non-genotoxic agents: predictive nature and comparison to lesions induced by genotoxic carcinogens. *Mutat Res* 1991; **248**: 239–60.
31 Kim H-N, Morimoto Y, Tsuda T *et al.* Changes in DNA 8-hydroxyguanine levels, 8-hydroxyguanine repair activity, and *hOGG1* and *hMTH1* mRNA expression in human lung alveolar epithelial cells induced by crocidolite asbestos. *Carcinogenesis* 2001; **22**: 265–9.
32 Hollenbach S, Dhenaut A, Eckert I, Radicella JP, Epe B. Overexpression of OGG1 in mammalian cells: effects on induced and spontaneous oxidative DNA damage and mutagenesis. *Carcinogenesis* 1999; **20**: 1863–8.
33 Bruner SD, Norman DPG, Verdine GL. Structural basis for recognition and repair of the endogenous mutagen 8-oxoguanine in DNA. *Nature* 2000; **403**: 859–66.
34 Kuznetsov NA, Koval VV, Zharkov DO, Nevinsky GA, Douglas KT, Fedorova OS. Kinetics of substrate recognition and cleavage by human 8-oxoguanine-DNA glycosylase. *Nucleic Acids Res* 2005; **33**: 3919–31.
35 Delker D, Hatch G, Allen J *et al.* Molecular biomarkers of oxidative stress associated with bromated carcinogenicity. *Toxicology* 2006; **221**: 158–65.
36 Nishimura S. Involvement of mammalian OGG1 (MMH) in excision of the 8-hydroxyguanine residue in DNA. *Free Rad Biol Med* 2002; **32**: 813–21.
37 Arai T, Kelly VP, Komoro K, Minowa O, Noda T, Nishimura S. Cell proliferation in liver of *Mmh/Ogg1*-deficient mice enhances mutation frequency because of the presence of 8-hydroxyguanine in DNA. *Cancer Res* 2003; **63**: 4287–92.
38 Kamiya H, Murata-Kamiya N, Koizume S, Inoue H, Nishimura S, Ohtsuka E. 8-Hydroxyguanine (7,8-dihydro-8-oxoguanine) in hot spots of the c-Ha-*ras* gene: effects of sequence contexts on mutation spectra. *Carcinogenesis* 1995; **16**: 883–9.
39 Jaloszynski P, Masutani C, Hanaoka F, Perez AB, Nishimura S. 8-Hydroxyguanine in a mutational hotspot of the c-Ha-*ras* gene causes misreplication, 'action-at-a-distance' mutagenesis and inhibition of replication. *Nucleic Acids Res* 2003; **31**: 6085–95.
40 Dybdahl M, Risom L, Moller P *et al.* DNA adduct formation and oxidative stress in colon and liver Big Blue rats after dietary exposure to diesel particles. *Carcinogenesis* 2003; **24**: 1759–66.
41 Fujikawa K, Kamiya H, Kasai H. The mutations induced by oxidatively damaged nucleotides, 5-formyl-dUTP and 5-hydroxy-dCTP, in Escherichia coli. *Nucleic Acids Res* 1998; **26**: 4582–7.
42 Wallace SS. Biological consequences of free radical-damaged DNA bases. *Free Rad Biol Med* 2002; **33**: 1–14.
43 Tanaka T, Iwasa Y, Kondo S, Hiai H, Toyokuni S. High incidence of allelic loss on chromosome 5 and inactivation of $p15^{INK4B}$ and $p16^{INK4A}$ tumor suppressor genes in oxystress-induced renal cell carcinoma of rats. *Oncogene* 1999; **18**: 3793–7.
44 Umemura T, Takagi A, Sai K, Hasegawa R, Kurokawa Y. Oxidative DNA damage and cell proliferation in kidneys of male and female rats during 13-weeks exposure to potassium bromate ($KBrO_3$). *Arch Toxicol* 1998; **72**: 264–9.
45 Umemura T, Sai K, Takagi A, Hasegawa R, Kurokawa Y. A possible role for oxidative stress in $KBrO_3$ carcinogenesis. *Carcinogenesis* 1995; **16**: 593–7.
46 Umemura T, Kurokawa Y. Etiology of bromated-induced cancer and possible modes of action-studies in Japan. *Toxicology* 2006; **221**: 154–7.

Deletion and single nucleotide substitution at G:C in the kidney of *gpt* delta transgenic mice after ferric nitrilotriacetate treatment

Li Jiang,[1] Yi Zhong,[1] Shinya Akatsuka,[1] Yu-Ting Liu,[1] Khokon Kumar Dutta,[1] Wen-Hua Lee,[1] Janice Onuki,[1,2] Ken-ichi Masumura,[3] Takehiko Nohmi[3] and Shinya Toyokuni[1,4]

[1]Department of Pathology and Biology of Diseases, Graduate School of Medicine, Kyoto University, Kyoto 606-8501; [2]Laboratory of Biochemistry and Biophysics, Butantan Institute, São Paulo, SP, Brazil; [3]Division of Genetics and Mutagenesis, National Institute of Health Sciences, Tokyo 158-8501, Japan

(Received June 7, 2006/Revised July 13, 2006/Accepted July 14, 2006/Online publication August 23, 2006)

An iron chelate, ferric nitrilotriacetate (Fe-NTA), induces oxidative renal proximal tubular damage that subsequently leads to a high incidence of renal cell carcinoma in rodents, presenting an intriguing model of free radical-induced carcinogenesis. In the present study, we used *gpt* delta transgenic mice, which allow efficient detection of point mutations and deletions *in vivo*, to evaluate the mutation spectra, in association with the formation of 8-oxoguanine and acrolein-modified adenine during the first 3 weeks of carcinogenesis. Immunohistochemical analysis revealed the highest levels of 8-oxoguanine and acrolein-modifed adenine in the renal proximal tubules after 1 week of repeated administration. DNA immunoprecipitation and quantitative polymerase chain reaction analysis showed that the relative abundance of 8-oxoguanine and acrolein-modified adenine at the *gpt* reporter gene were increased at the first week in the kidney. Similarly, in both 6-thioguanine and Spi$^-$ selections performed on the renal specimens after Fe-NTA administration, the mutant frequencies were increased in the Fe-NTA-treated mice at the first week. Further analyzes of 79 mutant clones and 93 positive plaques showed a high frequency of G:C pairs as preferred targets for point mutation, notably G:C to C:G transversion-type mutation followed by deletion, and of large-size (>1 kilobase) deletions with short homologous sequences in proximity to repeated sequences at the junctions. The results demonstrate that the iron-based Fenton reaction is mutagenic *in vivo* in the renal tubular cells and induces characteristic mutations. (*Cancer Sci* 2006; 97: 1159–1167)

Oxidative stress is associated with a variety of pathological phenomena, including infection, inflammation, ultraviolet- and γ-irradiation, overload of transition metals and certain chemical agents.[1] Many epidemiological studies have demonstrated a close association between chronically oxidative conditions and carcinogenesis. For example, chronic tuberculous pleuritis causes a high incidence of malignant lymphoma;[2] asbestosis (asbestos fibers are rich in iron),[3] is often associated with mesothelioma and lung carcinoma;[4] chronic *Helicobacter pylori* infection is associated with a high incidence of gastric cancer;[5,6] the incidence of colorectal cancer is increased in ulcerative colitis;[7,8] a high risk for heptocellular carcinoma is observed in patients with genetic hemochromatosis, an iron overload disease;[9,10] severe burns by ultraviolet radiation is a risk factor for skin cancer;[11,12] and γ-irradiation causes a high incidence of leukemia.[13] At least under these circumstances, and probably in other types of carcinogenesis as well, oxidative stress appears to play a major role in human carcinogenesis.

An iron chelate, ferric nitrilotriacetate (Fe-NTA), causes oxidative renal proximal tubular injury via the Fenton reaction, and this injury ultimately leads to a high incidence of renal cell carcinoma in mice[14] and rats[15] after repeated intraperitoneal administration. This is an intriguing model in the following respects: (1) more than half of the induced tumors metastasize to the lung and/or invade the peritoneal cavity, resulting in animal mortality;[16] (2) convincing evidence exists regarding the involvement of free radical reactions in the carcinogenic process, including not only an increase in covalently modified macromolecules (oxidatively modified DNA bases[17] and lipid peroxidation products)[18,19] but also preventive effects of α-tocopherol fortification against carcinogenesis;[20] (3) genetic changes in the $p16^{INK4a}$ tumor suppressor gene, especially homozygous deletions[21,22] and expressional alteration of several key genes, including annexin 2[23] and thioredoxin binding protein-2,[24] have been observed.

Fe-NTA itself is Ames test-negative,[14] but is positive in other cell culture systems detecting mutations.[25,26] Thus far, its mutation spectrum has not been comprehensively studied. Since the Ames test is a system involving prokaryotes, an assay system with the ability to detect mutations under *in vivo* conditions in which eukaryotic DNA repair mechanisms, metabolic pathways and other physiological systems are operative would offer significant advantages with respect to reliability. Based on this premise, several transgenic mouse mutagenesis assay systems have been developed, including Muta mice,[27] Big Blue mice[28] and HITEC mice.[29] These systems employ a recoverable transgenic lambda phage vector containing a reporter gene from bacteria. However, these systems all have the limitation that large deletions cannot be efficiently detected. We have developed a novel mutagenesis test system named *gpt* delta transgenic mice, which are transgenic for the *lambda EG 10* gene containing the *gpt* gene of *Escherichia coli*.[30] An important feature of this system is that both point mutations and large deletions can be tested concurrently in the targeted organs of the mice; point mutations are detected by 6-thioguanine (6-TG) selection and deletions larger than 1 kb can be identified by Spi$^-$ (sensitive to P2 interference) selection. Thus far, various mutagens, including γ-ray irradiation, UVB, mitomycin C and PhIP, have been studied by using this *in vivo* system.[31]

In the present study, we used *gpt* transgenic mice to investigate the early genetic changes in Fe-NTA-induced renal carcinogenesis. Furthermore, we studied the relative abundance of two different types of DNA base modifications in several limited genomic loci with a novel technique called DNA immunoprecipitation (DnaIP), which selectively collects enzyme-digested DNA fragments

[4]To whom correspondence should be addressed.
E-mail: toyokuni@path1.med.kyoto-u.ac.jp
Abbreviations: acrolein-dA, acrolein-modified 2′-deoxyadenosine; APNH, aminophenylnorharman; bp, base pairs; Cm, chloramphenicol; dCTP, 2′-deoxycytidine triphosphate; DnaIP, DNA immunoprecipitation; EDTA, ethylenediaminetetraacetic acid; FaPy, formamidopyrimidine; Fe-NTA, ferric nitrilotriacetate; MF, mutant frequency; MMC, mitomycin C; 8-OHdG, 8-hydroxy-2′-deoxyguanosine; PCR, polymerase chain reaction; PhIP, 2-amino-1-methyl-6-phenylimidazo[4,5-b]pyridine; 6-TG, 6-thioguanine; UVB, ultraviolet B; TE, Tris-EDTA.

doi: 10.1111/j.1349-7006.2006.00301.x

containing the target oxidative DNA base modification with specific monoclonal antibody. The present study for the first time revealed characteristics of the mutation spectrum in the kidney following repeated episodes of the Fenton reaction.

Materials and Methods

Animals and chemicals. *Gpt* delta C57BL/6 J transgenic mice were provided by Dr Takehiko Nohmi (Division of Genetics and Mutagenesis, National Institute of Health Sciences, Tokyo, Japan) and maintained in Kyoto University under specific-pathogen free and light-, temperature- and humidity-controlled conditions. The animal experiment committee of the Graduate School of Medicine, Kyoto University, approved the present experiments. $Fe(NO_3)_3 9H_2O$ was obtained from Wako (Osaka, Japan). Nitrilotriacetic acid, disodium salt, was purchased from Nacalai Tesque (Kyoto, Japan). Fe-NTA was prepared immediately before use as described previously.[18] A total of 12 4-week-old male mice were used; nine mice were subjected to repetitive Fe-NTA administration and three mice were used as untreated controls. Mice were injected intraperitoneally with 3 mg iron/kg of Fe-NTA daily for three days, and the dose was increased to 5 mg iron/kg of Fe-NTA from the fourth day according to the established carcinogenesis protocol.[16] The injections were performed five times a week at approximately 10.00 hours. The animals were killed 48 h after the final administration. Both kidneys and the central lobe of the liver were immediately excised. Half of one kidney and a portion of the liver were used for histological and immunohistochemical analysis, and the rest of the kidney was frozen in liquid nitrogen and stored at −80°C for mutational analyzes.

Monoclonal antibodies. Monoclonal antibody N45.1 recognizing 8-hydroxy-2′-deoxyguanosine (8-OHdG)[32] and monoclonal antibody mAb21 recognizing acrolein-2′-deoxyadenosine adduct (acrolein-dA)[33] were used.

Histological and immunohistochemical analyzes. Kidney specimens were fixed with phosphate-buffered 10% formalin and embedded in paraffin, cut at 3-μm thickness and stained with hematoxylin and eosin staining. For immunohistochemical analyzes, the avidin-biotin complex method with peroxidase was used as described previously.[32,33]

DNA immunoprecipitation and quantitative PCR analysis. To evaluate the relative abundance of Fe-NTA-induced oxidative DNA base modifications (8-OHdG and acrolein-dA) at desired genomic loci, we developed a technique designated as DnaIP (DNA immunoprecipitation).[34] More details will be published elsewhere.[35] Briefly, genomic DNA was extracted from each kidney of *gpt* delta transgenic mice with the NaI method (Wako) using argon gas-saturated buffer to avoid further oxidation during the extraction procedures.[36] Twenty μg of genomic DNA was digested with *Hae*III (TakaraBio, Shiga, Japan), and incubated with each antibody (10 μg of N45.1 or 2 μg of mAb21) in 10 mM phosphate-buffered saline, pH 7.4, containing 0.1% bovine serum albumin, for 3 h at 4°C in a 900-μL volume. The mixture was then incubated with 100 μL of Dynabeads M-280 sheep antimouse IgG (Dynal, Oslo, Norway) for another 3 h, washed sequentially with four different buffers (buffer 1: 0.1% sodium deoxycholate, 1% Triton X-100, 1 mM EDTA, 50 mM HEPES-KOH, 140 mM NaCl, pH 7.5; buffer 2: 0.1% sodium deoxycholate, 1% Triton X-100, 1 mM EDTA, 50 mM HEPES-KOH, 500 mM NaCl, pH 7.5; buffer 3: 0.1% sodium deoxycholate, 0.5% Nonidet P-40, 1 mM EDTA, 250 mM LiCl, 10 mM Tris-HCl, pH 8.0; and buffer 4: 1 × TE). Beads-bound DNA was recovered by incubating the beads with 80 μL of elution buffer (10 mM EDTA, 1% SDS, 50 mM Tris-HCl, pH 8.0) at 65°C for 10 min, and was amplified twice by PCR after ligation to an adaptor (sense, 5′-OH-GGAATTCGGCGGCCGCGGATCC-3′; antisense, 5′-GGATCC-GCGGCCGCCG-3′; sense oligonucleotides were used as primers for amplification), treated with exonuclease I (TakaraBio) and purified with phenol-chloroform extraction. The purified products were subjected to Real-Time PCR (7300 Real Time PCR System, Applied Biosystems, Tokyo) using Platinum SYBR Green qPCR SuperMix UDG (Invitrogen, Tokyo). The primer pairs used were as follows: *gpt*, forward-5′-GCCTTCTGAACAATGGAAAGG-3′, reverse-5′-CGTGATCGTAGCTGGAAATAC-3′ (125 bp); β-*actin*, forward-5′-TCCAACAAACCAAGAGAAATCC-3′, reverse-5′-CGACCTCTGAAACAATTCTGGT-3′ (108 bp); C15-49–5 (chromosome 15, extrageneic region), forward-5′-TGGTACCTGAGT-AAGGCAAGGT-3′, reverse-5′-CCCACTTGTGATTGCTTTCTTC-3′ (107 bp); C16-47–2 (chromosome 16, extrageneic region): forward-5′-CACACACACATGCACACTGTACT-3′, reverse-5′-GCATTTCTCCTCACATTCAGACT-3′ (114 bp); C16-47–5 (chromosome 16, extrageneic region): forward-5′-CCAATTGG-AGCTAACAGAAACC-3′, reverse-5-AGCTGGTCAACTGCC-TACTCTC-3′ (125 bp). These three extrageneic areas were selected based on our observations that chromosome 15 is peripherally located and chromosome 16 is centrally located in the murine renal tubular cells at interphase.[35]

***In vitro* phage packaging.** Genomic DNAs were extracted with the phenol-chloroform extraction protocol.[37] Trangenic *lambda EG10* DNA was rescued from the host genomic DNA using Transpack Packaging Extract (Stratagene, La Jolla, CA) according to the manufacturer's instructions.[30]

Mutation analysis. The 6-TG mutation assay protocol has been described elsewhere.[38–40] Briefly, rescued phage was infected into YG 6020 *E. coli* expressing Cre enzyme, converted into a plasmid carrying the *Cm-resistance* gene and *gpt* gene, and poured on plates containing chloramphenicol (Cm) with or without 6-TG. The positive clones carrying the mutant *gpt* gene were obtained from 6-TG selection plates by incubating at 37°C for 96 h. Selected clones were confirmed again by plating on 6-TG selection plates. The whole *gpt* sequence was amplified from positive clones and identified by sequencing with an ABI PRIZM 377 sequencer. The primers used for amplifying and sequencing were as follows: forward-5′-GCGCAACCTATTTTCCCCTCGA-3′ and reverse-5′-TGGAAACTATTGTAACCCGCCTG-3′. The same primer pair was used for direct sequencing.[41] *E. coli* XL1-Blue MRA and XL1-Blue MRA (P2) were infected with the packaged phage. *E. coli* XL1-Blue MRA was poured onto NZY plates and XL1-Blue MRA (P2) was poured onto I-trypticase agar plates. Plaques that grew on the XL1-Blue MRA (P2) plates were selected and further confirmed with *E. coli* XL1-Blue MRA, *E. coli* WL95 (P2) and XL1-Blue MRA (P2). Positive plaques were recovered and used for determining the deletion position of the *red/gam* gene. Clones or plaques were counted for determining mutant frequencies (MFs). MFs were calculated by using established methods as described previously.[30,42,43]

Hybridization assay and PCR analysis for Spi⁻ mutant analysis. A protocol for Southern blot analysis for Spi⁻ (sensitive to P2 interference) mutants has been established.[43] Seventeen oligomers located within ~14 kb flanking sequence of the *red/gam* gene were used as probes for identifying the deletion junctions. These oligomers were named 18874R, 19258R, 20341R, 21328R, 22556R, 22869R, 23921R, 24858R, 25389F, 26704F, 27096F, 28165F, 29290F, 30104F, 31070F, 31879F and 32890F according to their position as described.[43] The oligomers were spotted onto Hybond™-N⁺ membrane (Amersham) and cross-linked with UV. PCR products, which were amplified by primer 18874R and 32890F using positive individual plaques as templates, were labeled with (α-^{32}P) dCTP using the Megaprime DNA labeling System (Amersham). The membranes were incubated with labeled PCR products at 50°C overnight, washed three times and exposed to BioMax film (Kodak, New York, NY). Deleted regions were located within those oligomers whose signals could not be observed on the film. The nearest primers were selected for PCR amplification and the PCR products were subjected to sequencing to determine the exact deletion junction.

doi: 10.1111/j.1349-7006.2006.00301.x

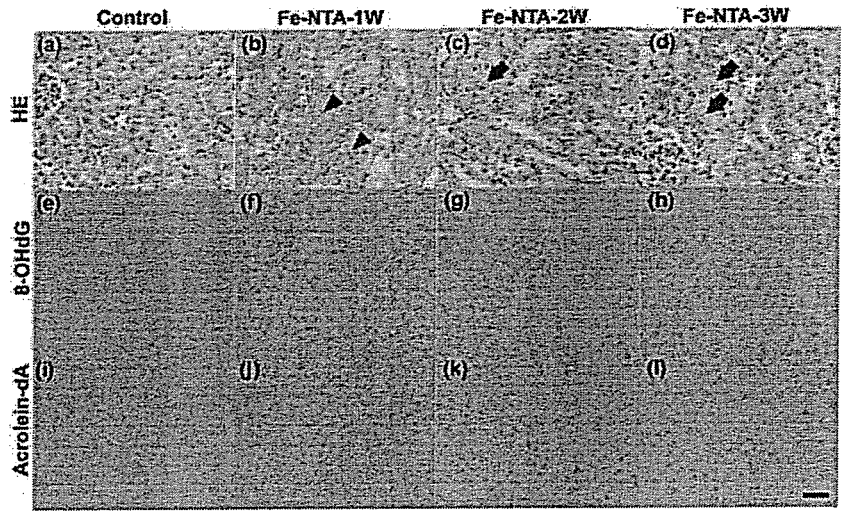

Fig. 1. Immunohistochemical analysis of 8-hydroxy-2'-deoxyguanosine (8-OHdG) and acrolein-modified 2'-deoxyadenosine after repeated administration of ferric nitrilotriacetate (Fe-NTA). (a–d) Hematoxylin and eosin (HE) staining. Regenerative proximal tubular cells were prominent at the first week, together with some necrotic cells (b, ▲). At the second and third week, necrotic cells were no longer observed but increasing numbers of karyomegalic cells (c and d, ▲) appeared. (e–h) Immunohistochemistry of 8-OHdG. Nuclear immunopositivity was observed after Fe-NTA administration, with the highest level after repeated administration for 1 week (f). (i–l) Immunohistochemistry of acrolein-dA. Nuclear immunopositivity was observed after Fe-NTA administration with that of repeated administration of 1 week the highest level (j). Refer to the Materials and Methods section for details (bar in l, 50 μm).

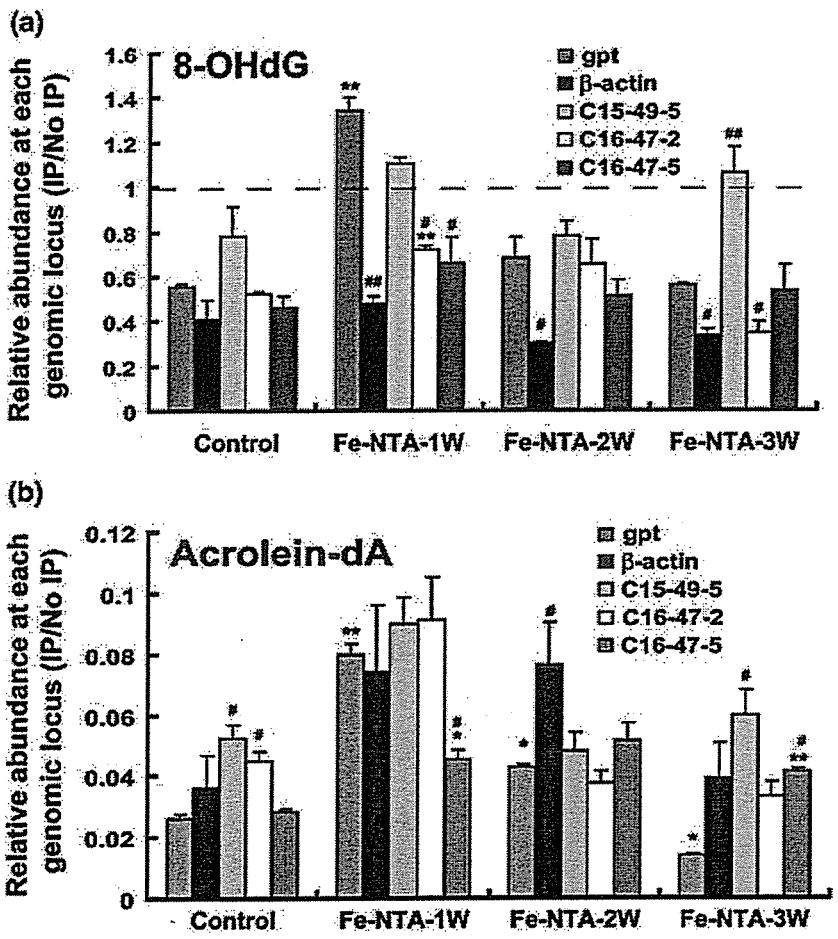

Fig. 2. Real-time polymerase chain reaction (RT-PCR) analysis after DNA immunoprecipitation for quantitation of oxidatively modified DNA bases at specific genomic loci. Renal genomic DNA was digested with *Hae*III and subjected to immunoprecipitation (IP) with specific monoclonal antibodies against 8-hydroxy-2'-deoxyguanosine (8-OHdG) and acrolein-dA. The recovered DNA fragments were amplified after ligation to an adapter and were used as substrates for RT-PCR analyses of *gpt*, β-*actin* and three extrageneic regions at chromosome 15 or 16. Data are shown as relative abundance of PCR products amplified from recovered genomic DNA by IP per those amplified from the original genomic DNA in the same amounts. (a) 8-OHdG. (b) Acrolein-dA. Refer to the Materials and Methods section for details ($N = 3$, means ± SEM; $^{*}P < 0.05$, $^{**}P < 0.01$ versus untreated control kidney at the same genomic region; $\#P < 0.05$, $\#\#P < 0.01$ versus *gpt* locus data of the same treatment group).

Statistical analysis. Statistical analyzes were performed with an unpaired *t*-test, which was modified for unequal variances when necessary.

Results

Renal histology after repeated Fe-NTA administration. As shown in Fig. 1a, no significant histological changes were observed in the kidney of the untreated control group. In contrast, pyknotic nuclei of proximal tubular cells revealing degeneration were scattered in the kidney of mice after 1 week of Fe-NTA treatment (Fig. 1b). Degenerative tubular cells were no longer observed there after 2 or 3 weeks of repeated Fe-NTA treatment, but atypical regenerative cells with a large nucleus containing prominent nucleoli were gradually increased (Fig. 1c,d). In either case, histological evaluation of the liver showed no apparent alterations (data not shown).

Oxidative DNA damage induced by repeated Fe-NTA administration. Two major oxidative DNA base modifications, 8-OHdG and acrolein-dA, were evaluated with immunohistochemistry and DnaIP. Intense diffuse nuclear immunostaining of 8-OHdG and acrolein-dA was prominent in the renal proximal tubules after repeated Fe-NTA administration for 1 week, and gradually decreased thereafter (Fig. 1e–l). To assess whether these oxidative modifications were increased in the *gpt* gene locus, quantitative PCR analysis after DnaIP was performed. The *gpt* reporter gene locus after 1 week of repeated Fe-NTA administration showed higher amounts of 8-OHdG and acrolein-dA than that in the untreated control group. Similar patterns were also observed in the other loci examined, but the *gpt* locus was the most sensitive at the first week (Fig. 2), consistently with the immunohistochemical data (Fig. 1e–l).

Fe-NTA-induced mutant frequencies in *gpt* and *red/gam* genes. We then investigated the reporter genes, *gpt* and *red/gam*, to analyze Fe-NTA-induced mutations using the 6-TG and Spi$^-$ selection systems. In both 6-TG and Spi$^-$ selections, the mutation frequencies were significantly increased (2.44-fold increase in 6-TG selection and 1.72-fold increase in Spi$^-$ selection) after 1 week of repeated Fe-NTA administration (Fig. 3), which was consistent with the results of immunohistochemistry (Fig. 1e–l) and DnaIP (Fig. 2).

Fe-NTA-induced *gpt* gene mutations. To further characterize the exact *gpt* mutations caused by Fe-NTA, 79 mutant clones, in which 69 clones were from Fe-NTA-treated mice and 10 from untreated control mice, were analyzed (Table 1 and Fig. 4). Among the mutations induced by Fe-NTA, 75.4% (52/69) were single base substitutions, of which more than half (32/52 = 61.5%) occurred at G:C base pairs, whereas GC content of *gpt* gene was 46.6%. Among the Fe-NTA-induced substitutions, 40.4% (21/52) were transitions, including G:C to A:T (13/21) and A:T to G:C (8/21), whereas the rest of substitutions (31/52 = 59.6%) were transversions, including G:C to T:A (5/31), G:C to C:G (14/31), A:T to T:A (4/31) and A:T to C:G (8/31) (Table 1). In addition, 17.4% (12/69) of mutant clones were identified as carrying single- or mutiple-base deletions. Among them, 9/12 were single-base deletions, which occurred preferentially at repeated sequences (Table 1 and Fig. 4). Four insertional mutations and one tandem base substitution were also observed. In contrast, analyses of a total of 10 clones from the untreated control kidney showed that 8/10 were single-base substitutions with a single-base deletion and an insertion. In either case, complex mutations were not observed. Therefore, the results indicated that Fe-NTA-induced *gpt* gene mutation preferentially consisted of single-base substitutions occurring at G:C base pairs, in which transversions were more frequent than transitions (Table 1).

Fe-NTA-induced Spi$^-$ mutations. To characterize the Spi$^-$ mutations induced by Fe-NTA, 93 positive plaques obtained from either the kidneys of Fe-NTA-treated mice or untreated control mice were screened by Southern blot analysis followed by sequencing that resulted in the confirmation of 21 large-size deletions (Fig. 5a). Large-size deletions were at first roughly positioned on ~14 kb of sequence spanning the *red/gam* gene by the use of 17 different oligomers as probes. We detected signals for all the 17 oligomer probes in the blot with hybridization to the wild-type *lambda EG 10* (Fig. 5b i). Signals for certain oligomers were absent with Spi$^-$ mutant plaques containing large-size deletions, as shown in Fig. 5(b ii–iv). Most of the large deletions induced by Fe-NTA were more than 1 kb in size (Class I mutation,[31] (Fig. 5a). Furthermore, the majority of them (70.6%) had short homologous sequences of 1–6 bp at the junctions (Class I-A), and in many cases showed three bp or longer running sequences at the junction or its vicinity. Five cases of large-size deletions were accompanied by simultaneous single-base deletion in the *red/gam* gene (Fig. 5a).

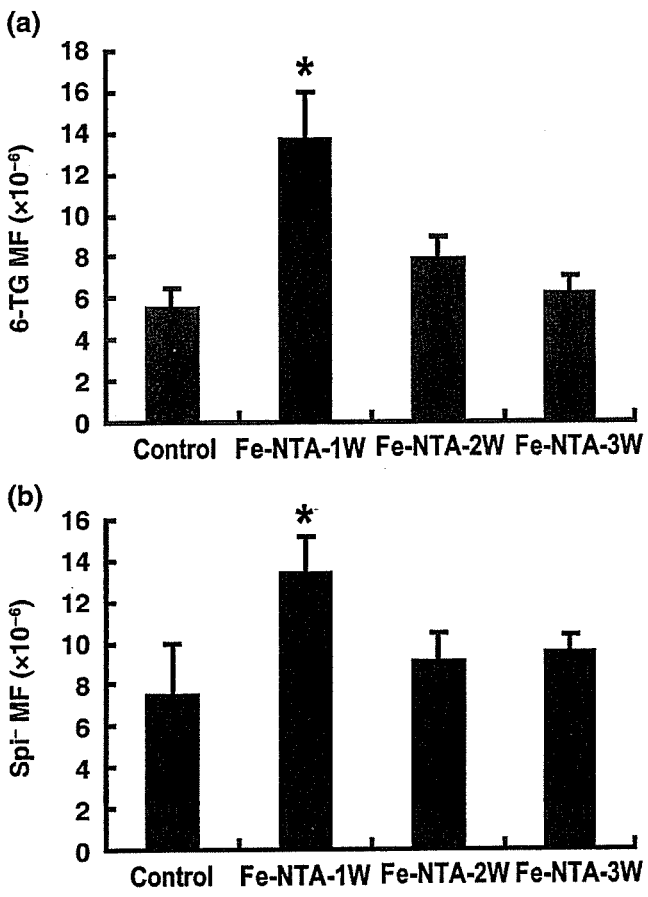

Fig. 3. Mutant frequency (MF) of 6-TG and Spi$^-$ seletion. 6-TG selection was used for the detection of base substitutions in the *gpt* gene; Spi$^-$ selection was used for the detection of large-size deletions. Refer to the Materials and Methods section for details. ($N = 3$, means ± SEM; $^*P < 0.05$, $^{**}P < 0.01$ *versus* untreated control kidney).

Discussion

In the present experiments we have for the first time studied the mutation spectrum of the Fenton reaction-based renal tubular damage in a model of oxidative stress-induced carcinogenesis mediated by Fe-NTA. We intentionally avoided the acute periods for evaluation because of the abundance of necrosis and apoptosis,[20,44] and thus used the subacute phase when the majority of the tubular cells become resistant to oxidative stress with rare cell death present (Fig. 1b–d), though mutation spectrum might be slightly different between the acute and subacute phases. The accumulation of two different kinds of oxidative DNA base modifications, 8-OHdG and acrolein-dA, was most evident with immunohistochemistry after the first week of repeated administration of Fe-NTA and gradually decreased thereafter (Fig. 1e–l). This is probably due to the activation in the cellular metabolic pathways for those either suppressing the Fenton reaction or promoting DNA repair mechanisms. It is also possible that cellular selective processes worked to remove heavily damaged cells.

Gpt delta transgenic mice are an established model for analyzing mutations *in vivo*, and have been used to analyze several possible mutagens.[31] Here we have used a technique designated as DnaIP to evaluate the relative abundance of the two DNA base modifications at the *gpt* loci. Approximately 80 copies of the

doi: 10.1111/j.1349-7006.2006.00301.x

Table 1. Spectrum of Fe-NTA-induced mutations in the kidney of *gpt* delta transgenic mice

Mutation type	Nucleotide position	Sequence change	Amino acid change	Fe-NTA 1w	Fe-NTA 2w	Fe-NTA 3w	Control
Transition					30.4%		50.0%
G:C–A:T	27	G–A	Trp–STOP	1			
	39	G–A	Gln–Gln				1
	64	C–T	Arg–STOP	1			1
	110	G–A	Arg–His	5			1
	113	G–A	Arg–His				1
	116	G–A	Arg–Arg			1	
	128	G–A	Val–Met		1	1	
	287	C–T	Thr–Ile	1			
	356	G–A	Arg–His		1		
	447	C–T	Ile–Ile			1	
A:T–G:C	2	T–C	Met–Thr		1		
	25	T–C	Trp–Ser	1	2		
	188	A–G	Tyr–Cys		1		
	275	A–G	Asp–Gly				1
	307	A–G	Met–Val	1			
	410	A–G	Gln–Arg		1		
	415	T–C	Trp–Arg			1	
Transversion					44.9%		30.0%
G:C–T:A	3	G–T	Ser–Ile		1		
	110	G–T	Arg–His		1		
	115	G–T	Gly–Cys	1			
	189	C–A	Tyr–STOP	1			
	324	C–A	His–Gln				1
	418	G–T	Asp–Try	1			
G:C–C:G	109	C–G	Arg–Gly			1	
	125	C–G	Pro–Arg			1	
	238	G–C	Asp–His			1	
	297	G–C	Ala–Ala	2			
	413	C–G	Pro–Arg	2	1		
	414	G–C	Pro–Pro	2			
	427	G–C	Val–Leu	1		1	
	430	G–C	Val–Leu	2			1
A:T–T:A	52	A–T	Lys–STOP	1			
	66	A–T	Arg–Arg			1	
	179	T–A	Ile–Asn		1	1	
A:T–C:G	94	A–C	Ile–Leu		1		
	133	T–G	Phe–Val		1		
	134	T–G	Gly–STOP		1	1	
	146	A–C	Glu–Ala		1		
	286	A–C	Thr–Pro	1		1	
	315	A–C	Pro–Pro	1			
	375	T–G	Tyr–STOP				1
Deletions					17.4%		10.0%
1 base pair	8–12	AAAAA–AAAA		1	3	1	1
	88–90	AAAGG–AAGG				1	
	423–425	GGGCG–GGCG		1			
	430	TCGTA–TCTA				1	
	437	CGTCC–CGCC				1	
>2 base pairs	156–162	ATTCGTCATGT–ATCG			1		
	170–171	TACCG–TAG			1		
	252–253	TTCATC–TTTC			1		
Insertions					5.7%		10.0%
	74–75	CCTT–CCAATT				1	
	122–123	GTAC–GTTAC		1			
	310–311	ATCC–ATTCC			1	1	
	440–441	CCGC–CCCGC					1
Other					1.4%		0.0%
CC–AG	124–125	TACCGG–TAAGGG			1		

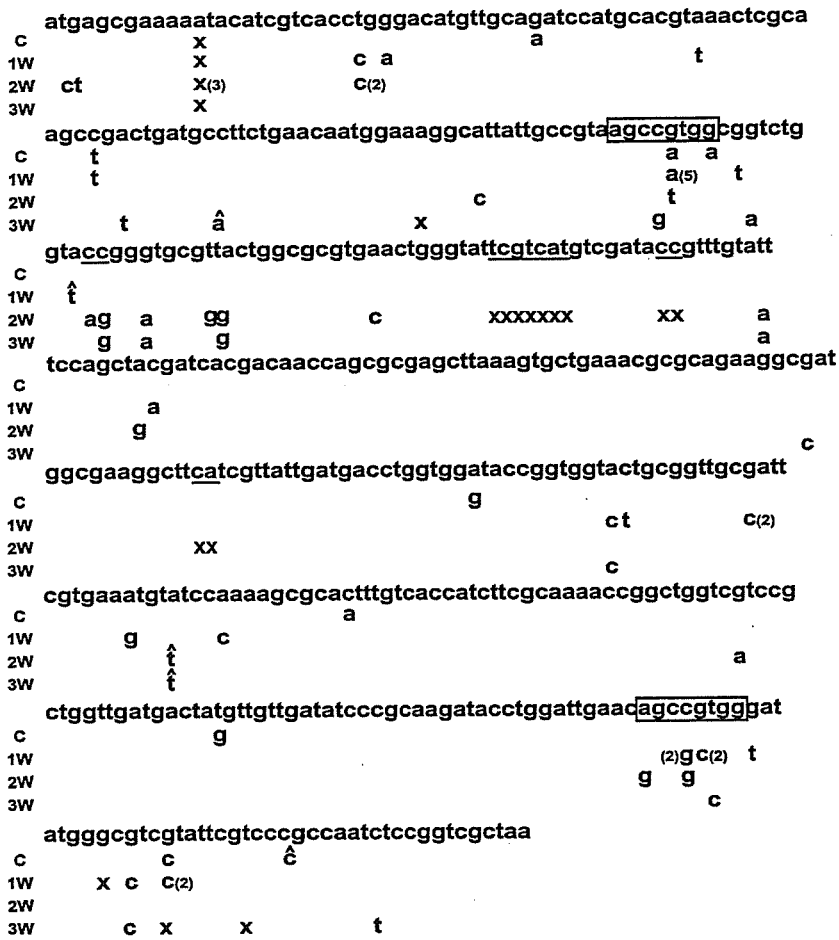

Fig. 4. The position of point mutations in the *gpt* gene. Refer to the Materials and Methods section for details (x, deletion; ^, insertion; underline, more than one base pair deletion within the same case; the number in parenthesis indicates the multiplicity of the same mutation. Square (in one letter), mutation-prone area with the same sequence.

transgenes are included per haploid genome in the *gpt* delta transgenic mice.[30] Among genomic loci examined, including β-actin and three extrageneic regions, the *gpt* loci showed the highest level of 8-OHdG and acrolein-dA after one week of repeated Fe-NTA administration (Fig. 2). This consistency with the immunohistochemical data demonstrates that the transgenic *gpt* loci are indeed vulnerable and suitable for mutational analyzes. We believe that the high copy number of the *gpt* gene contained in these mice is at least partially responsible for this reliable sensitivity. In contrast to the findings at one week, certain extrageneic loci showed significantly higher levels of DNA base modifications than the *gpt* gene locus at other time points, suggesting that further studies would be necessary to elucidate the principles governing the distribution of oxidative DNA base modifications over the whole genome.[35,45]

Mutation frequencies both for the 6-TG selection and Spi$^-$ selection also were the highest at the first week of repeated Fe-NTA administration (Fig. 3). This confirms the usefulness of 8-OHdG and acrolein-dA, which were detected both by immunohistochemistry and DnaIP, as reliable markers of mutation. In 22.7% of the Spi$^-$ plaques after Fe-NTA treatment, large-size deletions (>1 kb) were observed and most of them were class I-A mutants (Fig. 5). This preference for large-size deletions with short homologous sequences at the junctions might be a prominent feature of the results obtained in this renal carcinogenesis model in that the patterns of Spi$^-$ mutations are similar to that of the untreated colon.[31] With γ-rays, shorter deletions than 1 kb are prominent; with UVB and MMC, large-size deletions with or without short homologous sequences at the junctions are more frequently observed (>40%); whereas with PhIP and APNH, large-size deletions were rare.[31]

In the Fe-NTA-induced renal cell carcinoma of rats, homozygous deletion of the *p16^{INK4A}* tumor suppressor gene was frequently observed,[21] and the allelic loss of this locus was observed at a high frequency one to three weeks after the repeated administration of Fe-NTA in rats.[22] We believe that the iron-mediated Fenton reaction is mainly responsible for this characteristic deletion. Short deletions were also increased after Fe-NTA administration (Table 1). Probably, the free radical reaction associated with iron is distinct from the reactions associated with other agents studied so far in the *gpt* lambda transgenic mice in that this is a universal reaction, though exaggerated through iron overload, involving the generation of hydroxyl radical and lipid peroxidation products. This kind of reaction is always taking place in the body under conditions of normal metabolism associated with oxygen consumption and, though it results in only minor consequences under physiological conditions, can be a driving force of carcinogenesis.

The mutation spectrum detected in the *gpt* gene was also quite distinctive. G:C pairs were the preferred bases for mutation, and especially G:C to C:G transversion-type mutation was characteristic (Fig. 4 and Table 1). This type of mutation was observed in PhIP and MMC as a minor type, but has not been reported as a major type of mutation (Table 2). We observed a low incidence of G:C to T:A transversion-type mutation that results from

doi: 10.1111/j.1349-7006.2006.00301.x

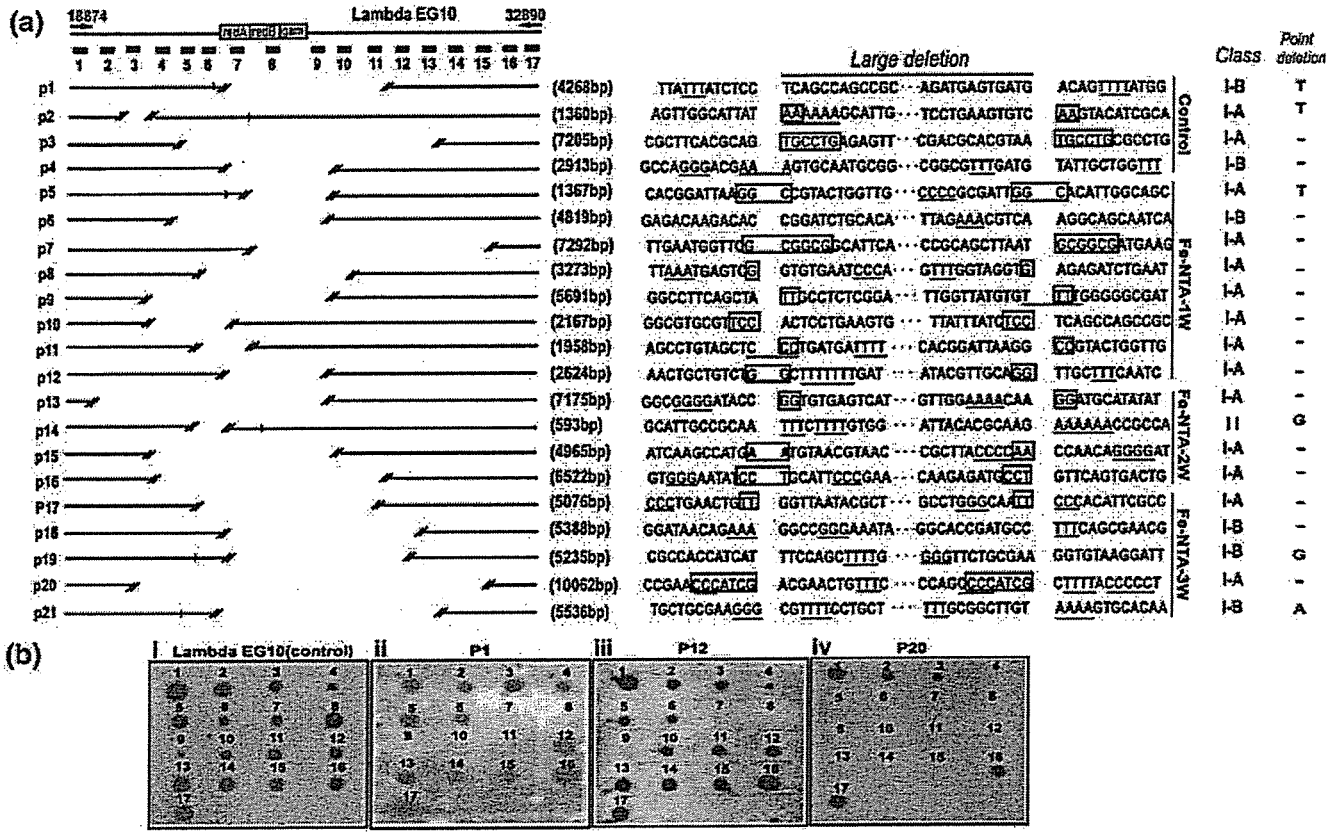

Fig. 5. Size and position of large-size deletions after Spi⁻ selection with each junctional sequence. (a) Summary of the strategy and the observed deletions. P1–P4, untreated control; P5–P21, ferric nitrilotriacetate (Fe-NTA)-induced deletions. Blank areas between two double-dash lines indicate large-size deletions; short longitudinal lines indicate accompanying 1-base deletion; □, short homologous sequence; underline, short run more than 3 bp. Classification of the deletion type was done as described.[31] (b) Representative results of Southern blotting analysis for screening the deleted positions. Arabic numerals (1–17) indicate the probes used as described in the Materials and Methods section and P1, P12 and P20 correspond to the a section.

8-OHdG formation.[46,47] This may be explained by the fact that this mutagenic process is strongly inhibited by a DNA repair enzyme, Mutyh.[48] Here we may propose a mechanism in which certain oxidative modification to guanine/cytosine may cause abnormal pairing with the same corresponding base. Recently, it was reported that formamidopyrimidine (FaPy)-guanine, another oxidative DNA base modification,[49,50] would not be responsible for this type of mutation.[51] We suspect that 5,6-dihydroxyuracil and 5-hydroxycytosine which are increased in this model[17] or other aldehyde-modified bases than acrolein-dA are among the possible candidates.

When we reviewed the spectrum of point mutation observed in the *p53*, *tsc2*, *p15*, *p16 and tbp-2* tumor suppressor genes of Fe-NTA-induced rat renal carcinoma, we observed no G:C to C:G transversions, but G:C to T:A (*p53*, *tbp-2*),[16,24] T:A to C:G (*tsc2*), G:C to A:T (*p15 and p16*, *tbp-2*),[21] A:T to T:A (*tbp-2*)[24] and one nucleotide insertion/deletion at repeat sequences (*p16*, *tbp-2*)[21,24] were observed despite the limited available data. There are at least several possibilities to explain this: (i) we have not yet identified the target genes with G:C to C:G mutations; (ii) there are some species-differences between mice and rats; (iii) this mutation spectrum detected in this *gpt* transgenic system is largely reflected in non-geneic genome areas; and (iv) the last possibilities are that G:C to C:G mutations are preferentially repaired by mismatch repair enzyme(s) in non-transgene areas or abundant mutations of this kind lead to lethal effects, affecting fundamental transcriptional activity in the expressed genes. Regarding species differences, another study using the *gpt* delta transgenic rat[52] would answer the question. The data obtained with DnaIP is of note in that 8-OHdG and acrolein-dA were increased in some non-geneic regions after three weeks of repeated administration of Fe-NTA, warranting further studies.

In conclusion, we used the *gpt* delta transgenic mice to evaluate the mutation spectrum of the Fenton reaction-based oxidative renal tubular injury, and found that the major mutations consist of large-size deletions with short homologous sequences at the junctions and transversion-type point mutations at G:C base pairs. The mutant frequency was the highest at the first week of repeated Fe-NTA administration, as shown by the immunohistochemistry of 8-OHdG and acrolein-dA as well as the presence of these two modified bases at the *gpt* loci, indicating that this early stage is one of the critical periods in this Fenton reaction-induced carcinogenesis.

Acknowledgments

This work was supported in part by a Grant-in-Aid from the Ministry of Education, Culture, Sports, Science and Technology of Japan, a Grant-in-Aid for Cancer Research from the Ministry of Health, Labour and Welfare of Japan, and a grant of Long-range Research Initiative (LRI) by Japan Chemical Industry Association (JCIA).

Table 2. **Comparison of mutations induced by various mutagens in *gpt* delta transgenic mice**

Target	Kidney†				Bone marrow[38]		Colon[39]	
	Control (MF = 1.0)	Fe-NTA-1 W (MF = 2.4)	Fe-NTA-2 W (MF = 1.4)	Fe-NTA-3 W (MF = 1.1)	Control (MF = 1.0)	PhIP (MF = 10.9)	Control (MF = 1.0)	ENU (MF = 3.2)
G:C–A:T	40%	28.6% (1.72)	8.7% (0.30)	16.7% (0.46)	43.1%	14.1%	26.9%	28.3%
A:T–G:C	10%	7.1% (1.70)	21.7% (3.04)	5.6% (0.62)	11.1%	0.0%	3.8%	20.0%
G:C–T:A	10%	10.7% (2.57)	8.7% (1.21)	0% (0.00)	26.4%	52.5%	11.5%	15.0%
G:C–C:G	10%	32.1% (7.70)	4.3% (0.60)	22.2% (2.44)	0.0%	13.1%	7.7%	0.0%
A:T–T:A	0%	3.6% (∞)	4.3% (∞)	11.1% (∞)	5.6%	1.0%	3.8%	28.3%
A:T–C:G	10%	7.1% (1.70)	17.4% (2.44)	11.1% (0.62)	4.2%	0.0%	0.0%	5.0%
Deletion	10%	7.1% (1.70)	26.1% (3.65)	22.2% (2.44)	4.2%	15.1%	38.5%	3.3%
Insertion	10%	3.6% (0.86)	4.3% (0.60)	11.1% (1.22)	5.6%	1.0%	7.7%	0.0%
Others	0%	0.0% (NA)	4.3% (∞)	0.0% (NA)	0.0%	3.0%	0.0%	0.0%

Target	Bone marrow[41]		Liver[53]		Liver[54]		Epidermis[55]		Liver[56]	
	Control (MF = 1.0)	MCC (MF = 2.9)	Control (MF = 1.0)	APNH (MF = 10.3)	Control (MF = 1.0)	γ-ray (MF = 3.2)	Control (MF = 1.0)	UVB (MF = 7.7)	Control (MF = 1.0)	MeIQx (MF = 8.6)
G:C–A:T	24.1%	13.3%	41%	23%	27%	20%	64%	87%	43%	16%
A:T–G:C	3.4%	6.7%	10%	1%	15%	0%	0%	3%	8%	0%
G:C–T:A	31.0%	26.7%	14%	51%	12%	25%	9%	0%	10%	54%
G:C–C:G	10.3%	6.7%	2%	1%	4%	0%	0%	1%	4%	5%
A:T–T:A	6.9%	3.3%	8%	0%	4%	0%	9%	4%	8%	3%
A:T–C:G	10.3%	3.3%	4%	0%	23%	10%	10%	0%	2%	0%
Deletion	13.8%	6.7%	18%	16%	12%	35%	18%	0%	12%	16%
Insertion	0.0%	0.0%	2%	0%	4%	10%	0%	0%	2%	0%
Others	0.0%	33.3%	2%	7%	0%	0%	0%	5%	11%	6%

†present study. The number in parenthesis is the relative mutation frequency in comparison to the untreated control. MF, mutation frequency; NA, not applied; W, week(s); Fe-NTA, ferric nitrilotriacetate; PhIP, 2-amino-1-methyl-6-phenylimidazo [4,5-b]pyridine; ENU, ethylnitrosourea; MMC, mitomycin C; APNH, aminophenylnorharman; UVB, ultraviolet B; MeIQx, 2-amino-3,8-dimethylimidazo[4,5-f]quinoxaline.

References

1 Halliwell B, Gutteridge JMC. *Free radicals in biology and medicine*. Oxford: Clarendon Press, 1999.
2 Iuchi K, Ichimiya A, Akashi A *et al.* Non-Hodgkin's lymphoma of the pleural cavity developing from long-standing pyothorax. *Cancer* 1987; **60**: 1771–5.
3 Gilmour P, Brown D, Beswick P, MacNee W, Rahman I, Donaldson K. Free radical activity of industrial fibers: role of iron in oxidative stress and activation of transcription factors. *Environ Health Perspect* 1997; **105** (Suppl 5): 1313–17.
4 Hodgson J, Darnton A. The quantitative risks of mesothelioma and lung cancer in relation to asbestos exposure. *Ann Occup Hyg* 2000; **44**: 565–601.
5 Uemura N, Okamoto S, Yamamoto S *et al. Helicobacter pylori* infection and the development of gastric cancer. *N Engl J Med* 2001; **345**: 784–9.
6 Naito Y, Yoshikawa T. Carcinogenesis and chemoprevention in gastric cancer associated with *helicobacter pylori* infection: role of oxidants and antioxidants. *J Clin Biochem Nutr* 2005; **36**: 37–49.
7 Collins R, Feldman M, Fordtran J. Colon cancer, dysplasia, and surveillance in patients with ulcerative colitis. A critical review. *N Engl J Med* 1987; **316**: 1654–8.
8 Eaden J, Abrams K, Mayberry J. The risk of colorectal cancer in ulcerative colitis: a meta-analysis. *Gut* 2001; **48**: 526–35.
9 Toyokuni S. Iron-induced carcinogenesis: the role of redox regulation. *Free Radic Biol Med* 1996; **20**: 553–66.
10 Elmberg M, Hultcrantz R, Ekbom A *et al.* Cancer risk in patients with hereditary hemochromatosis and in their first-degree relatives. *Gastroenterology* 2003; **125**: 1733–41.
11 Grodstein F, Speizer F, Hunter D. A prospective study of incident squamous cell carcinoma of the skin in the nurses' health study. *J Natl Cancer Inst* 1995; **87**: 1061–6.
12 Nishigori C, Hattori Y, Toyokuni S. Role of reactive oxygen species in skin carcinogenesis. *Antioxid Redox Signal* 2004; **6**: 561–70.
13 Preston D, Kusumi S, Tomonaga M *et al.* Cancer incidence in atomic bomb survivors. Part III. Leukemia, lymphoma and multiple myeloma, 1950–87. *Radiat Res* 1994; **137**: S68–97.
14 Li JL, Okada S, Hamazaki S, Ebina Y, Midorikawa O. Subacute nephrotoxicity and induction of renal cell carcinoma in mice treated with ferric nitrilotriacetate. *Cancer Res* 1987; **47**: 1867–9.
15 Ebina Y, Okada S, Hamazaki S, Ogino F, Li JL, Midorikawa O. Nephrotoxicity and renal cell carcinoma after use of iron- and aluminum-nitrilotriacetate complexes in rats. *J Natl Cancer Inst* 1986; **76**: 107–13.
16 Nishiyama Y, Suwa H, Okamoto K, Fukumoto M, Hiai H, Toyokuni S. Low incidence of point mutations in *H-*, *K-* and *N-ras* oncogenes and *p53* tumor suppressor gene in renal cell carcinoma and peritoneal mesothelioma of Wistar rats induced by ferric nitrilotriacetate. *Jpn J Cancer Res* 1995; **86**: 1150–8.
17 Toyokuni S, Mori T, Dizdaroglu M. DNA base modifications in renal chromatin of Wistar rats treated with a renal carcinogen, ferric nitrilotriacetate. *Int J Cancer* 1994; **57**: 123–8.
18 Toyokuni S, Uchida K, Okamoto K, Hattori-Nakakuki Y, Hiai H, Stadtman ER. Formation of 4-hydroxy-2-nonenal-modified proteins in the renal proximal tubules of rats treated with a renal carcinogen, ferric nitrilotriacetate. *Proc Natl Acad Sci USA* 1994; **91**: 2616–20.
19 Toyokuni S, Luo XP, Tanaka T, Uchida K, Hiai H, Lehotay DC. Induction of a wide range of $C_{2\text{-}12}$ aldehydes and $C_{7\text{-}12}$ acyloins in the kidney of Wistar rats after treatment with a renal carcinogen, ferric nitrilotriacetate. *Free Radic Biol Med* 1997; **22**: 1019–27.
20 Zhang D, Okada S, Yu Y, Zheng P, Yamaguchi R, Kasai H. Vitamin E inhibits apoptosis, DNA modification, and cancer incidence induced by iron-mediated peroxidation in Wistar rat kidney. *Cancer Res* 1997; **57**: 2410–14.
21 Tanaka T, Iwasa Y, Kondo S, Hiai H, Toyokuni S. High incidence of allelic loss on chromosome 5 and inactivation of $p15^{INK4B}$ and $p16^{INK4A}$ tumor suppressor genes in oxystress-induced renal cell carcinoma of rats. *Oncogene* 1999; **18**: 3793–7.
22 Hiroyasu M, Ozeki M, Kohda H *et al.* Specific allelic loss of $p16^{INK4A}$ tumor suppressor gene after weeks of iron-mediated oxidative damage during rat renal carcinogenesis. *Am J Pathol* 2002; **160**: 419–24.
23 Tanaka T, Akatsuka S, Ozeki M, Shirase T, Hiai H, Toyokuni S. Redox regulation of annexin 2 and its implications for oxidative stess-induced renal carcinogenesis and metastasis. *Oncogene* 2004; **23**: 3980–9.
24 Dutta KKN, Ishinaka Y, Masutani H *et al.* Thioredoxin-binding protein-2 is a target gene in oxidative stress-induced renal carcinogenesis. *Lab Invest* 2005; **85**: 798–807.
25 Nakatsuka S, Tanaka H, Namba M. Mutagenic effects of ferric nitrilotriacetate (Fe-NTA) on V79 Chinese hamster cells and its inhibitory effects on cell-cell communication. *Carcinogenesis* 1990; **11**: 257–60.

doi: 10.1111/j.1349-7006.2006.00301.x

26 Toyokuni S, Sagripanti JL, Hitchins VM. Cytotoxic and mutagenic effects of ferric nitrilotriacetate on L5178Y mouse lymphoma cells. *Cancer Lett* 1995; **88**: 157–62.
27 Gossen J, de Leeuw W, Tan C *et al.* Efficient rescue of integrated shuttle vectors from transgenic mice: a model for studying mutations in vivo. *Proc Natl Acad Sci USA* 1989; **86**: 7971–5.
28 Kohler S, Provost G, Fieck A *et al.* Spectra of spontaneous and mutagen-induced mutations in the *lacI* gene in transgenic mice. *Proc Natl Acad Sci USA* 1991; **88**: 7958–62.
29 Gondo Y, Shioyama Y, Nakao K, Katsuki M. A novel positive detection system of in vivo mutations in *rpsL* (*strA*) transgenic mice. *Mutat Res* 1996; **360**: 1–14.
30 Nohmi T, Katoh M, Suzuki H *et al.* A new transgenic mouse mutagenesis test system using Spi⁻ and 6-thioguanine selections. *Environ Mol Mutagen* 1996; **28**: 465–70.
31 Nohmi T, Masumura K. Molecular nature of intrachromosomal deletions and base substitutions induced by environmental mutagens. *Environ Mol Mutagen* 2005; **45**: 150–61.
32 Toyokuni S, Tanaka T, Hattori Y *et al.* Quantitative immunohistochemical determination of 8-hydroxy-2′-deoxyguanosine by a monoclonal antibody N45.1: its application to ferric nitrilotriacetate-induced renal carcinogenesis model. *Lab Invest* 1997; **76**: 365–74.
33 Kawai Y, Furuhata A, Toyokuni S, Aratani Y, Uchida K. Formation of acrolein-derived 2′-deoxyadenosine adduct in an iron-induced carcinogenesis model. *J Biol Chem* 2003; **278**: 50 346–54.
34 Toyokuni S, Akatsuka S, Aung TT, Dutta KK. Free radical-induced carcinogenesis: target genes and fragile genome sites. *Free Radic Res* 2005; **39** (Suppl 1): S30.
35 Akatsuka S, Aung TT, Dutta KK *et al.* Contrasting genome-wide distribution of 8-hydroxyguanine and acrolein-modified adenine during oxidative stress-induced renal carcinogenesis. *Am J Pathol* 2006, in press.
36 Nakae D, Mizumoto Y, Kobayashi E, Noguchi O, Konishi Y. Improved genomic/nuclear DNA extraction for 8-hydroxydeoxyguanosine analysis of small amounts of rat liver tissue. *Cancer Lett* 1995; **97**: 233–9.
37 Ono T, Miyamura Y, Ikehata H *et al.* Spontaneous mutant frequency of *lacZ* gene in spleen of transgenic mouse increases with age. *Mutat Res* 1995; **338**: 183–8.
38 Masumura K, Matsui K, Yamada M *et al.* Mutagenicity of 2-amino-1-methyl-6-phenylimidazo [4,5-b]pyridine (PhIP) in the new *gpt* delta transgenic mouse. *Cancer Lett* 1999; **143**: 241–4.
39 Masumura K, Matsui M, Katoh M *et al.* Spectra of *gpt* mutations in ethylnitrosourea-treated and untreated transgenic mice. *Environ Mol Mutagen* 1999; **34**: 1–8.
40 Nohmi T, Suzuki T, Masumura K. Recent advances in the protocols of transgenic mouse mutation assays. *Mutat Res* 2000; **455**: 191–215.
41 Takeiri A, Mishima M, Tanaka K *et al.* Molecular characterization of mitomycin C-induced large deletions and tandem-base substitutions in the bone marrow of *gpt* delta transgenic mice. *Chem Res Toxicol* 2003; **16**: 171–9.
42 Cariello N, Piegorsch W, Adams W, Skopek T. Computer program for the analysis of mutational spectra: application to *p53* mutations. *Carcinogenesis* 1994; **15**: 2281–5.
43 Shibata A, Masutani M, Kamada N *et al.* Efficient method for mapping and characterizing structures of deletion mutations in *gpt* delta mice using Southern blot analysis with oligo DNA probes. *Environ Mol Mutagen* 2004; **43**: 204–7.
44 Hamazaki S, Okada S, Ebina Y, Midorikawa O. Acute renal failure and glucosuria induced by ferric nitrilotriacetate in rats. *Toxicol Appl Pharmacol* 1985; **77**: 267–74.
45 Toyokuni S, Akatsuka S. What has been learned from the studies of oxidative stress-induced carcinogenesis: proposal of the concept of oxygenomics. *J Clin Biochem Nutr* 2006; **39**: 3–10.
46 Shibutani S, Takeshita M, Grollman AP. Insertion of specific bases during DNA synthesis past the oxidation-damaged base 8-oxodG. *Nature* 1991; **349**: 431–4.
47 Kasai H. Analysis of a form of oxidative DNA damage, 8-hydroxy-2′-deoxyguanosine, as a marker of cellular oxidative stress during carcinogenesis. *Mutat Res* 1997; **387**: 147–63.
48 Nakabeppu Y. Regulation of intracellular localization of human MTH1, OGG1, and MYH proteins for repair of oxidative DNA damage. *Prog Nucl Acid Res Mol Biol* 2001; **68**: 75–94.
49 Steenken S. Purine bases, nucleosides, and nucleotides: aqueous solution redox chemistry and transformation reactions of their radical reactions and e⁻ and. OH adducts. *Chem Rev* 1989; **89**: 503–20.
50 Dizdaroglu M. Chemical determination of free radical-induced damage to DNA. *Free Radic Biol Med* 1991; **10**: 225–42.
51 Ober M, Muller H, Pieck C, Gierlich J, Carell T. Base pairing and replicative processing of the formamidopyrimidine-dG DNA lesion. *J Am Chem Soc* 2005; **127**: 18 143–9.
52 Hayashi H, Kondo H, Masumura K, Shindo Y, Nohmi T. Novel transgenic rat for *in vivo* genotoxicity assays using 6-thioguanine and Spi⁻ selection. *Environ Mol Mutagen* 2003; **41**: 253–9.
53 Masumura K, Totsuka Y, Wakabayashi K, Nohmi T. Potent genotoxicity of aminophenylnorharman, formed from non-mutagenic norharman and aniline, in the liver of *gpt* delta transgenic mouse. *Carcinogenesis* 2003; **24**: 1985–93.
54 Masumura K, Kuniya K, Kurobe T, Fukuoka M, Yatagai F, Nohmi T. Heavy-ion-induced mutations in the *gpt* delta transgenic mouse: comparison of mutation spectra induced by heavy-ion, X-ray, and gamma-ray radiation. *Environ Mol Mutagen* 2002; **40**: 207–15.
55 Horiguchi M, Masumura K, Ikehata H *et al.* UVB-induced *gpt* mutations in the skin of *gpt* delta transgenic mice. *Environ Mol Mutagen* 1999; **34**: 72–9.
56 Masumura K, Horiguchi M, Nishikawa A *et al.* Low dose genotoxicity of 2-amino-3,8-dimethylimidazo[4,5-f]quinoxaline (MeIQx) in *gpt* delta transgenic mice. *Mutat Res* 2003; **541**: 91–102.

Genes and Environment, Vol. 28, No. 3 pp. 84–91 (2006)

Regular article

Chemopreventive Effects of Nobiletin against Genotoxicity Induced by 4-(Methylnitrosamino)-1-(3-pyridyl)-1-butanone (NNK) in the Lung of *gpt* delta Transgenic Mice

Megumi Ikeda[1,2], Ken-ichi Masumura[1], Keiko Matsui[1], Hiroyuki Kohno[3], Keiko Sakuma[2], Takuji Tanaka[3] and Takehiko Nohmi[1,4]

[1]Division of Genetics and Mutagenesis, National Institute of Health Sciences, Tokyo, Japan,
[2]Graduate School of Nutrition and Health Sciences, Kagawa Nutrition University, Saitama, Japan,
[3]Department of Oncologic Pathology, Kanazawa Medical University, Ishikawa, Japan

(Received May 22, 2006; Revised June 8, 2006; Accepted June 15, 2006)

Nobiletin, a major component of citrus polymethoxyflavones, possesses anticancer, antiviral and anti-inflammatory activities. To evaluate the chemopreventive potential against lung cancer induced by cigarette smoke, we examined suppressive effects of nobiletin against genotoxicity induced by 4-(methylnitrosamino)-1-(3-pyridyl)-1-butanone (NNK), the most carcinogenic tobacco-specific nitrosamine, in the lung of *gpt* delta transgenic mice. Male and female *gpt* delta mice were fed nobiletin at a dose of 100 or 500 ppm in diet for seven days and treated with NNK at a dose of 2 mg/mouse/day, i.p. for four consecutive days. Dietary administration of nobiletin continued at the doses during the NNK treatments and in the following period before sacrifice at day 38. NNK treatments enhanced the *gpt* mutant frequency (MF) in the lung 19- and 9-fold, respectively, over the values of untreated female and male mice. Interestingly, nobiletin reduced the NNK-induced MFs by 25–45% in both sexes and the reduction at a dose of 100 ppm in females and 500 ppm in males was statistically significant ($P<0.05$). To further characterize the suppressive effects, we conducted bacterial mutation assay with *Salmonella typhimurium* YG7108 to examine whether nobiletin inhibits S9-mediated genotoxicity of NNK. Nobiletin as well as 8-methoxypsoralen, an inhibitor of CYP2A, reduced the genotoxicity of NNK by more than 50%. These results suggest that nobiletin may be chemopreventive against NNK-induced lung cancer and also that the chemopreventive efficacy may be due to inhibition of certain CYP enzymes involved in the metabolic activation of NNK.

Key words: nobiletin, NNK, chemoprevention, cigarette smoking, *gpt* delta transgenic mice

Introduction

Humans are exposed to a variety of exogenous and endogenous genotoxic agents. Of various hazardous environmental factors, cigarette smoke may be the most causative factor associated with the incidence of human cancer (1). Although cigarette smoke contains more than 4,000 compounds including 40 known human carcinogens, 4-(methylnitrosamino)-1-(3-pyridyl)-1-butanone (nicotine-derived nitrosamino ketone, NNK) is the most carcinogenic tobacco-specific nitrosamine (2,3). NNK is estimated to be present at levels of 17–430 and 390–1,440 ng, respectively, per cigarette in mainstream and sidestream of cigarette smoke (3). NNK induces lung tumors in rats, mice and hamsters and is classified into Class 2B carcinogen (possibly carcinogenic to humans) by International Agency for Research on Cancer (4). NNK is metabolically activated by CYP (P-450) enzymes, and the metabolites generate methylated and pyridyloxobutylated DNA, which can induce G:C-to-A:T and G:C-to-T:A mutations, respectively. O^6-Methylguanine in the lung may be a causative lesion of NNK leading to activation of Ki-*ras* protooncogene, an initiation of tumor development (5,6).

With smoking the major etiological factor for lung cancer, a number of naturally occurring and synthetic chemicals have been proposed as candidates of chemopreventive agents to protect smokers who are unwilling or unable to quit smoking. Examples of the candidates include inhibitors of metabolic activation of NNK, e.g., phenethyl isothiocyanate and curcumins (7–10), enhancers of detoxication enzymes, e.g., prodrugs of L-selenocystein (11), antioxidants, e.g., vitamine E and carotenoids (12,13) and inhibitors of signal transduction downstream from the activated oncogenes, e.g., perillyl alcohol and deguelin (14,15).

Nobiletin (5,6,7,8,3′,4′-hexamethoxyflavone) is a

[4]Correspondence to: Takehiko Nohmi, Division of Genetics and Mutagenesis, National Institute of Health Sciences, 1-18-1, Kamiyoga, Setagaya-ku, Tokyo 158-8501 Japan. Tel: +81-3-3700-9873, Fax: +81-3-3707-6950, E-mail: nohmi@nihs.go.jp

polymethoxyflavone found in *Citrus depressa* Rutaceae, a popular citrus fruit in Okinawa, Japan (16). Interestingly, nobiletin seems to possess anticancer activities by inhibiting critical steps of carcinogenesis, i.e., initiation (13,17), promotion (18,19) and metastasis (16,20,21). In addition, nobiletin inhibits the P-glycoprotein drug efflux transporter, suggesting the ability to reverse multi-drug resistance of tumor cells (22).

To evaluate the chemopreventive efficacy against lung cancer induced by cigarette smoke, we examined suppressive effects of dietary administration of nobiletin in the lung of *gpt* delta mice treated with NNK. In this mouse model, base substitutions such as G:C-to-A:T or G:C-to-T:A can be detected by *gpt* selection. In fact, Miyazaki *et al.* (23) have employed the mice to demonstrate the chemopreventive effects of 8-methoxypsoralen against NNK-induced mouse lung adenoma. Besides *in vivo* genotoxicity assays, we conducted a bacterial mutation assay with *Salmonella typhimurium* YG7108 to examine whether nobiletin inhibits the genotoxicity of NNK in the presence of S9 metabolic activation system. The bacterial strain lacks O^6-methylguanine methyltransferase activity, so that it is highly sensitive to base substitution mutations by NNK and other alkylating agents (24,25). The results suggest that nobiletin clearly suppresses the genotoxicity of NNK *in vivo* and *in vitro*. We discuss the mechanisms underlying the suppressive effects and the possible usage of nobiletin as a chemopreventive agent against lung cancer induced by cigarette smoke.

Material and Methods

Materials: Nobiletin (>99.9% purity) was chemically synthesized according to the method described by Tsukayama *et al.* (26) with slight modifications. Sources of other chemicals used in this study are as follows: NNK, Toronto Research Chemicals (Toronto, Canada); benzo[a]pyrene (BP), Wako Pure Chemicals (Osaka, Japan); 8-methoxypsoralen and *N*-methyl-*N'*-nitro-*N*-nitrosoguanidine (MNNG), Sigma-Aldrich Japan K. K. (Tokyo, Japan). S9 prepared from male Sprague-Dawley rats pretreated with phenobarbital and 5,6-benzoflavone was purchased from Kikkoman Cooperation, Chiba, Japan.

Treatment of *gpt* delta mice: Male and female *gpt* delta C57BL/6J transgenic mice, obtained from Japan SLC, Inc. (Shizuoka, Japan), were maintained in Animal Facility of Kanazawa Medical University, according to the institutional animal care guidelines. The animals were housed in plastic cages with free access to tap water and powdered basal diet CRF-1 (Oriental Yeast, Tokyo, Japan) under controlled conditions of temperature at 23±2°C, humidity of 10% and lighting (12 h light-dark cycle). Twenty female and 25 male *gpt* delta mice were each divided into four experimental and one control groups (Fig. 1). When the mice were 8 weeks of age, they were fed diet supplemented with nobiletin at a concentration of 100 ppm (Group 2) or 500 ppm (Groups 3 and 4) for 38 days. Groups 1 through 3 were treated with a single i.p. injection of NNK dissolved in saline at a dose of 2 mg/mouse/day for four consecutive days from day 7 through day 10. Groups 4 and 5 were treated with saline as vehicle. Mice were sacrificed under ether anesthesia at day 38. The lung was removed, placed immediately in liquid nitrogen, and stored at −80°C until analysis.

DNA Isolation, *in vitro* packaging and *gpt* mutation assay: High-molecular-weight genomic DNA was extracted from the lung using the RecoverEase DNA Isolation Kit (Stratagene, La Jolla, CA). λEG10 phages were rescued using Transpack Packaging Extract (Stratagene, La Jolla, CA). The *gpt* mutation assay was performed according to previously described methods (27,28). *gpt* MFs were calculated by dividing the number of colonies growing on agar plates containing chloramphenicol and 6-thioguanine by the product of the number of colonies growing on plates containing chloramphenicol and the dilution factor.

Bacterial mutation assay: The mutagenicity assay was carried out with a pre-incubation method with modifications (29). Nobiletin or 8-methoxypsoralen was dissolved in DMSO and the solution (50 μL) was mixed with S9 mix (0.5 mL). They were kept on ice for 5 min and mixed with the solution (50 μL) of chemicals, i.e., NNK, BP or MNNG, dissolved in DMSO. Then, they were mixed with overnight culture (0.1 mL) and incubated for 20 min at 37°C. When the mutagenicity of MNNG was assayed, 1/15M phosphate buffer pH7.4 (0.5 mL) was added instead of S9 mix. The reaction mixture containing bacteria, nobiletin (or 8-methoxypsoralen) and the chemical with or without S9 mix was poured onto agar plates with soft agar and incubated for two days at 37°C. Each chemical was assayed with 6–8 doses on triplicate or duplicate plates. Tester strains for the mutation assays were *S. typhimurium* YG7108 for NNK and MNNG, and *S. typhimurium* YG5161 (30) for BP. Relevant genotypes of the strains are as follows: YG7108 (24,25) as *S. typhimurium* TA1535 but is Δada_{ST} Δogt_{ST}; YG5161 (30) as *S. typhimurium* TA1538 harboring plasmid pYG768 carrying the *dinB* gene of *Escherichia coli*.

Statistical analysis: All data are expressed as mean ± standard deviations. Differences between groups were tested for statistical significance using a Student's *t*-test. A *P* value less than 0.05 denoted the presence of a statistically significant difference.

Results

Dietary administration of nobiletin suppresses mutations induced by NNK in the lung of *gpt* delta mice: To examine the suppressive effects of nobiletin against genotoxicity induced by NNK, female and male *gpt* delta mice were fed nobiletin in diet at a dose of 100 or 500 ppm for a week and treated with NNK (Fig. 1). Dietary administration of nobiletin continued during the NNK treatments and in the following period before sacrifice at day 38. NNK treatments enhanced *gpt* MF in the lung 19 times in females and 9 times in males over the control levels (Tables 1 and 2). Since the MFs ($\times 10^{-6}$) of untreated controls were similar between females and males (3.0 ± 1.3 versus 3.1 ± 2.0), NNK-induced MF was higher in females (58.1 ± 16.7) than in males (26.5 ± 11.8). Nobiletin itself was non-genotoxic (Group 4). Nobiletin appeared to reduce the MFs in both sexes. In females, the dietary administration of nobiletin at 100 and 500 ppm (Groups 2 and 3) reduced the NNK-induced MF by 34 and 32%, respectively, and the reduction at 100 ppm was statistically significant ($P<0.04$). In males, nobiletin at 100 and 500 ppm reduced the MF by 25 and 45%, respectively, and the reduction at 500 ppm was statistically significant ($P<0.04$). These results indicate that nobiletin suppresses NNK-induced genotoxicity in the lung of *gpt* delta mice.

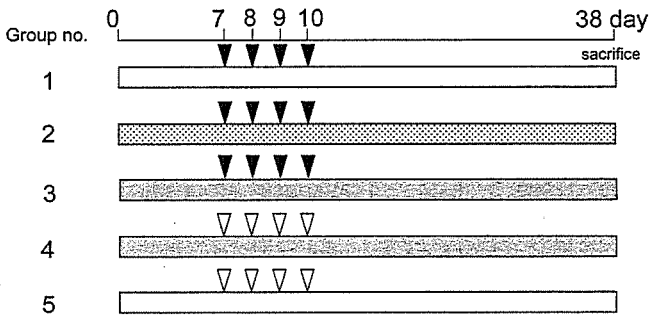

Fig. 1. An experimental design to examine chemopreventive effects of nobiletin against genotoxicity of NNK in the lung of *gpt* delta mice. Twenty female and 25 male eight-week-old *gpt* delta mice were each divided into five groups. Groups 1 through 3 were treated with a single i.p. injection of NNK at a dose of 2 mg/mouse/day for four consecutive days from day 7 through day 10. Groups 2 and 3 were fed diet supplemented with nobiletin at doses of 100 ppm and 500 ppm, respectively, for 38 days. Groups 4 and 5 were treated with saline as vehicle, and Group 4 was fed diet with nobiletin at a dose of 500 ppm for 38 days. Mice were sacrificed at day 38, and the *gpt* MF in the lung were determined. □, basal diet; ▨, nobiletin in diet at a dose of 100 ppm; ▩, nobiletin in diet at a dose of 500 ppm; ▼, NNK (2 mg/mouse/day, i.p.); ▽, saline.

Nobiletin inhibits genotoxicity of NNK in the presence of S9 activation in *S. typhimurium* YG7108: To further characterize the suppressive effects of nobiletin against genotoxicity of NNK, we conducted bacterial mutation assays to examine whether nobiletin inhibits genotoxicity of NNK in the presence of S9 activation enzymes (Fig. 2A). NNK at a dose of 500 μg/plate induced mutations in *S. typhimurium* YG7108 and produced about 900 His^+ revertants/plate, which was 40–50 times higher than the value of spontaneous mutations. Nobiletin itself was non-genotoxic either with or without S9 activation (Fig. 2A, C and D).

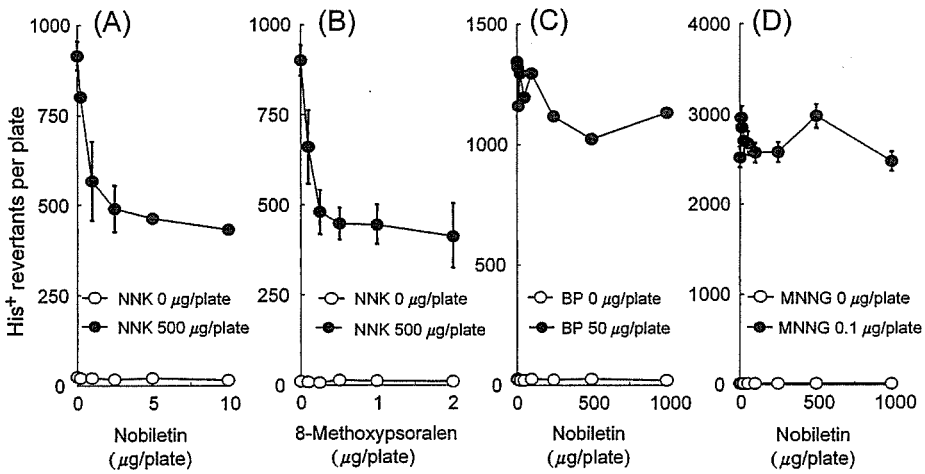

Fig. 2. Suppressive effects of nobiletin against genotoxicity of NNK in the presence of S9 mix in *S. typhimurium* YG7108. Closed circles represent the numbers of His^+ revertants/plate induced by the following compounds: NNK (500 μg/plate) in the presence of S9 mix along with the increasing doses of nobiletin (A), NNK (500 μg/plate) in the presence of S9 mix along with the increasing doses of 8-methoxypsoralen (B); BP (50 μg/plate) in the presence of S9 mix along with the increasing doses of nobiletin (C); MNNG (0.1 μg/plate) in the absence of S9 mix along with the increasing doses of nobiletin. Open circles represent the numbers of His^+ revertants/plate when the non-genotoxicity of nobiletin (A, C and D) and 8-methoxypsoralen (B) were confirmed. Strains used are *S. typhimurium* YG7108 (A, B and D) and *S. typhimurium* YG5161 (C). Averages and standard deviations are presented in A, B and D where three plates were used for the assays. Averages are presented in C where two plates were used for the assay.

Table 1. Suppressive effects of nobiletin against genotoxicity of NNK in the lung of female *gpt* delta mice

Group number*	Animal I.D.	Total colonies	No. of mutants	*gpt* MF ($\times 10^{-6}$)	Average ± S.D.†	*P*-value‡
1	F001	898,500	68	75.7		
NNK alone	F002	1,017,000	57	56.1		
	F003	1,464,000	53	36.2		
	F004	1,054,500	68	64.5		
		4,434,000	246	55.5	58.1 ± 16.7	
2	F005	1,134,000	36	31.8		
NNK	F006	1,353,000	48	35.5		
+ Nobiletin	F007	1,152,000	54	46.9		
(100 ppm)	F008	916,500	37	40.4		
		4,555,500	175	38.4	38.6 ± 6.6	0.036§
3	F009	1,369,500	33	24.1		
NNK	F010	798,000	36	45.1		
+ Nobiletin	F011	1,606,500	66	41.1		
(500 ppm)	F012	1,027,500	48	46.7		
		4,801,500	183	38.1	39.3 ± 10.4	0.052
4	F013	1,059,000	3	2.8		
Nobiletin	F014	1,377,000	4	2.9		
(500 ppm)	F015	1,092,000	6	5.5		
alone	F016	900,000	6	6.7		
		4,428,000	19	4.3	4.5 ± 1.9	< 0.001
5	F018	2,856,000	6	2.1		
No treatments	F019	1,560,000	4	2.6		
	F020	1,809,000	9	5.0		
	F021	2,013,000	5	2.5		
		8,238,000	24	2.9	3.0 ± 1.3	< 0.001

*Group 1, mice treated with NNK (2 mg/mouse/day × 4 days) alone; Group 2, mice treated with NNK plus nobiletin at a dose of 100 ppm in diet; Group 3, mice treated with NNK plus nobiletin at a dose of 500 ppm in diet; Group 4, mice fed nobiletin at a dose of 500 ppm in diet without NNK treatments; Group 5, mice without treatments with NNK or nobiletin. The Group No. corresponds with group No. in Fig. 1.

†Average ± standard deviation of *gpt* MF of four mice.

‡Differences between *gpt* MF of each group and that of Group 1 were tested for statistical significance using a Student's *t*-test.

§Statistically significant ($P < 0.05$) against Group 1. The values in Groups 4 and 5 are also statistically significant. But the mice in Groups 4 and 5 are not treated with NNK so that the values are not marked with §.

An addition of nobiletin in the reaction mixture containing NNK and S9 mix reduced the genotoxicity of NNK in a dose-dependent manner, and the number of His^+ revertants/plate decreased by more than 50% at the highest dose of nobiletin, i.e., 10 μg/plate. There was no obvious reduction of background lawn of bacteria at any dose of nobiletin, suggesting that nobiletin was not very much toxic under the experimental conditions. Similar dose-dependent reduction of the genotoxicity of NNK was observed with 8-methoxypsoralen (Fig. 2B). An addition of 8-methoxypsoralen into the reaction mixture containing NNK and S9 mix reduced the number of His^+ revertants/plate by more than 50%. Despite the similar inhibitory effects, the dose necessary to reduce the genotoxicity of NNK by 50% was 5- to 10-fold higher with nobiletin than with 8-methoxypsoralen (2.5 μg/plate for nobiletin versus 0.25–0.5 μg/plate for 8-methoxypsoralen). In contrast, nobiletin exhibited weak or virtually no inhibitory effects on the genotoxicity of BP or MNNG, respectively (Fig. 2C and D). An addition of nobiletin reduced the genotoxicity of BP in the presence of S9 activation by 20%, while it did not modulate the genotoxicity of MNNG in the absence of S9 enzymes.

Discussion

Lung cancer continues to be the leading cause of cancer death in developed countries. Dietary compounds with potential to inhibit lung cancer may be a promising and practical approach for reducing the risk of lung cancer caused by smoking. In this study, we examined the chemopreventive efficacy of nobiletin